

Integrated energy performance of an innovative translucent photoluminescent building envelope for lighting energy storage

Chiara Chiatti ^a, Federica Rosso ^{b,c,*}, Claudia Fabiani ^{a,d}, Anna Laura Pisello ^{a,d}

^a CIRIAF - Interuniversity Research Center, University of Perugia, Via G. Duranti 67, 06125, Perugia, Italy

^b Department of Civil and Environmental Engineering – University of Perugia, Via G. Duranti 97, 06125, Perugia, Italy

^c Department of Civil, Construction and Environmental Engineering - Sapienza University of Roma, Via Eudossiana 18, 00184, Roma, Italy

^d Department of Engineering – University of Perugia, Via G. Duranti 97, 06125, Perugia, Italy

ARTICLE INFO

Keywords:

Photoluminescent material
Energy efficiency
Lighting
Lighting energy storage
Building envelope
Cool material
Urban heat island

ABSTRACT

Novel, photoluminescent and translucent construction elements are considered for application on buildings' envelope toward energy savings and avant-garde architectural expression. These elements allow natural light to pass through the envelope and charge the materials, which on their turn re-emit energy as visible light. By exploiting the intrinsic characteristics of these construction elements large amounts of energy could be saved in lighting applications. This work tackles the complex, dynamic behavior of photoluminescent materials by means of a novel, experimental and numerical methodology. Materials' dynamic characteristics are firstly investigated by means of an in-lab experimental campaign. Secondly, coupled lighting and energy numerical simulations are carried out. Results show that translucent and photoluminescent envelope components could be able to reduce up to 40% building electricity consumption for lighting on an annual basis and depending on urban surroundings. In the best-case scenario, i.e. during the longest day of the year, the obtained electricity savings are around 80% for the photoluminescent–translucent envelope.

1. Introduction

The process of light transmission, absorption and reflection by a surface shapes human perception of the surrounding environment (Cai et al., 2018; Peeters, Smolders, & de Kort, 2020). Different materials interact differently with light throughout the solar spectrum. For instance, materials' color is the results of their interaction with the visible waveband in the solar spectrum. When light is reflected, the wavelength of the impinging ray is not changed by the interaction with the material's surface. In contrast, when light is absorbed, it is generally transformed into heat. Yet, there is a special class of materials that can emit visible light upon the absorption of a proper radiation wavelength, i.e. photoluminescent materials. Luminescence is the direct consequence of the absorption of energy by a material exposed to an adequate exciting source. Different types of luminescence can be distinguished, depending on the nature of the exciting radiation (Capelletti, 2017): for instance, we talk about bioluminescence if the light emission is caused by a biochemical reaction inside a living organism (e.g. plankton, jellyfish, etc.) (Kahlke & Umbers, 2016; Moline et al., 2009), while electroluminescence is the result of electricity passing through a substance (Chen & Shi, 1998; Gong et al., 2018).

The present research deals with photoluminescence, i.e. a phenomenon in which solid-state compounds emit light upon excitation by means of ultraviolet (UV) or visible (VIS) irradiation. According to the afterglow duration, which depends on the energy levels in the atomic structure of the compounds, photoluminescence is commonly distinguished in (i) fluorescence, if the light emission stops as the solicitation ends, or (ii) phosphorescence, if the material emanates light for a relatively longer time after the end of the exposure, as a kind of lighting storage system (Capelletti, 2017). This unique capability could be used in a large number of applications and it is, indeed, a promising research topic for both scientists and cutting-edge technology developers. In fact, the available literature on luminescent materials comprehends a wide variety of studies in which the luminous behavior of compounds is investigated as function of their chemical properties (Havasi, Sipos, Konya, & Kukovecz, 2020; Singh, Hakeem, & Lakshminarayana, 2020; Yousif, Abas, Shivaramu, & Swart, 2020). Efforts have been made by scientists to improve the photoluminescence performance in terms of both intensity and duration, focusing on the optimization of compounds' chemical formula, but the possible fields of application that

* Corresponding author at: Department of Civil, Construction and Environmental Engineering - Sapienza University of Roma, Via Eudossiana 18, 00184, Roma, Italy.

E-mail addresses: chiara.chiatti@crbnet.it (C. Chiatti), federica.rosso@uniroma1.it (F. Rosso), claudia.fabiani@unipg.it (C. Fabiani), anna.pisello@unipg.it (A.L. Pisello).

<https://doi.org/10.1016/j.scs.2021.103234>

Received 15 March 2021; Received in revised form 1 July 2021; Accepted 3 August 2021

Available online 10 August 2021

2210-6707/© 2021 Elsevier Ltd. All rights reserved.

best suit the obtained results remain just introduced and not deeper investigated. Starting from this, luminescent materials have gained increasing attention as a new category of cool materials, i.e. passive solutions with proper thermo-optical features able to counterbalance the increase in surface and air temperatures that is affecting urban areas during the last decades (Dimoudi et al., 2014; Gros, Bozonnet, & Inard, 2014; Levinson, Chen, Ferrari, Berdahl, & Slack, 2017; Santamouris & Yun, 2020; Zhao & Fong, 2017). The well-documented Urban Heat Island (UHI) phenomenon, is mainly caused by cities' layout (characteristics, materials, landscape, etc.) and local climate (Cheung & Jim, 2019; Tepanosyan et al., 2021). Highly-absorbing materials affect the city thermal balance by increasing the amount of sensible heat stored and released into the atmosphere, consequently intensifying local discomfort in the urban environment (Gilbert et al., 2017; He, Wang, Liu, & Ulpiani, 2021; Resch, Andresen, Cherubini, & Brattebø, 2021; Xu & Asawa, 2020). This leads to the exacerbation of energy consumption in buildings for heating and cooling purposes and to negative impacts on human comfort and health, even related to pollution increase (Ulpiani, 2021). For all these reasons, the study and development of both natural and artificial materials for UHI mitigation, characterized by optimal thermal-optical properties (i.e. high solar reflectance and high thermal emissivity) is a crucial topic (Gilbert, Mandel, & Levinson, 2016). Green and blue strategies have largely been investigated to counteract UHI (Tan, Sun, Huang, Yuan, & Hou, 2021). Parallel to these solutions, gray strategies, such as that of cool materials, have a prominent role in mitigating UHI phenomenon (Pigliautile, Châfer, Pisello, Pérez, & Cabeza, 2020; Qi, He, Wang, Zhu, & Fu, 2019) and decreasing energy consumption in buildings at the same time (Cabeza & Châfer, 2020).

In this context, investigations on the implementation of photoluminescent materials in real-scale engineering solutions are scarce. Only a few studies proposed their application as possible UHI mitigation strategies. Levinson et al. (2017), for example, showed how the temperature surface of ruby crystal samples was about 6.5 °C cooler than that of the non-fluorescent reference case, highlighting the benefit in the overall solar reflectance value of the material, due to fluorescence implementation. At a larger scale, Kousis, Fabiani, Gobbi, and Pisello (2020) carried out a monitoring campaign on concrete pavements integrating photoluminescent aggregates and finishing, obtaining a surface temperature reduction of about 3.3 °C and a non-negligible time delay during the summer period if compared to the performance of only concrete based surfaces. On the other hand, Rosso, Fabiani, Chiatti, and Pisello (2019) hypothesized the application of a photoluminescent paint on the external envelope of a case-study building and, through a dynamic energy simulation, assessed a summer temperature reduction of about 6 °C in the indoor environment. Moreover, given the ability of such materials to act as "lighting energy storage" (borrowing the definition from that of "thermal energy storage" Bilardo, Fraisse, Pailha, & Fabrizio, 2019; Borri, Zsembinszki, & Cabeza, 2021), their contribution as cost-free sources of lighting for both indoors and outdoors, during evening and night hours, deserves to be quantified in terms of energy consumption reduction. To this aim Fabiani, Chiatti, and Pisello (2021) explored the potential integration of photoluminescent components in outdoor environments, demonstrating the feasibility of combining active and passive lighting systems to meet standard requirements, reducing at the same time energy consumption and related costs.

The studies on the above testify to further optimize photoluminescent compounds for real-world applications within the built environment, but they also reveal the absence of a standardized characterization methodology taking into account the real boundary conditions triggering in-field photoluminescence (Chiatti, Fabiani and Pisello, 2021). In particular, the need to evaluate the type of irradiation activating the material's afterglow and its consequent decay time is fundamental, being both extremely sensitive to the local environment and application. For instance, in outdoors the irradiating source may be the sun and the material's time of exposure changes with seasons, while in indoors the exciting artificial light may be even tailored to perfectly

match the absorption waveband of the material. Following this line of research, Chiatti, Fabiani, Cotana and Pisello (2021) proposed an experimental methodology for the characterization of different types of photoluminescent materials, combining thermal and optical procedures for their classification as both cooling and energy saving solutions. Statistically analyzing the obtained data, they evaluated the impact of material composition and exposure boundary conditions. Despite their promising performance, to the best of the authors knowledge, no full scale investigation of the potential comprehensive energy saving performance of photoluminescent materials integration within building envelope solutions exists. Conversely, several studies have been focusing on the possible energy savings produced by translucent components and glazings (Rosso & Pisello, 2018). Rosso, Pisello, Cotana, and Ferrero (2017), for example, demonstrated the capability of thin, natural stone envelopes to diffuse natural light inside the building, which allowed to save 11% in electricity in a year. Similarly, Ahuja and Mosalam (2017) demonstrated that translucent concrete panels allow cutting down energy expenditure by 18%. Aerogel-based windows were the subject of numerous studies investigating the thermal-energy and lighting performance of such peculiar translucent construction material (Berardi, 2015; Gao, Ihara, Grynning, Jelle, & Lien, 2016; Garnier, Muneer, & McCauley, 2015). Integrated semi-transparent photovoltaic systems were considered for daylight performance, due to their translucent effect allowing light into the building (Fan, Yang, & Yang, 2020). Finally, Giovannini and colleagues (Giovannini, Goia, Lo Verso, & Serra, 2017) analyzed translucent Phase Change Materials-based glazing and assessed improvements in visual comfort of the occupants when overall luminance of visible sky is low.

1.1. Purpose of the study

Based on the above, the purpose of this study is to investigate for the first time the energy and lighting performance of photoluminescent-translucent envelopes in urban areas. In greater detail, the research questions (RQs) to be solved are the following:

- RQ1: How can photoluminescent and translucent materials contribute to building energy consumption reduction when employed as facades' components? Indeed, in consideration of the novelty of such photoluminescent materials, still a few applications, and even less scientific studies, dealt with their employment in buildings' facades.
- RQ2: Which is the contribution of photoluminescent and translucent materials in indoor lighting, and how can it be measured? In fact, given the peculiarity of the dynamic optic characteristics of photoluminescent materials, the performance of this kind of construction elements entails a complex analysis, which constitutes another original contribution of this work. In order to more precisely and punctually disclose the performance of these novel coupled photoluminescent-translucent materials, the here presented experimental and numerical analyses is purposely designed.

2. Materials and samples

In this work, the potential implementation of photoluminescent-translucent materials as components of the building envelope is proposed. The samples are commercially available glass-based square tiles of 10 cm side and 0.5 cm thickness, characterized by the addition of photoluminescent pigments, that make the material change its appearance according to the local boundary conditions, behaving as trigger for the photoluminescent activation. These tiles absorb solar radiation and re-emit it at longer-wavelengths for a limited amount of time. The mixture made of pigments and glass goes through a 3–6 h long firing process at about 600 °C–1200 °C, depending on the specific afterglow color and sample size. In particular, the sample selected for this study appears lobster-red-colored in its off phase, i.e. without the photoluminescent effect in progress (Fig. 1a), while it turns

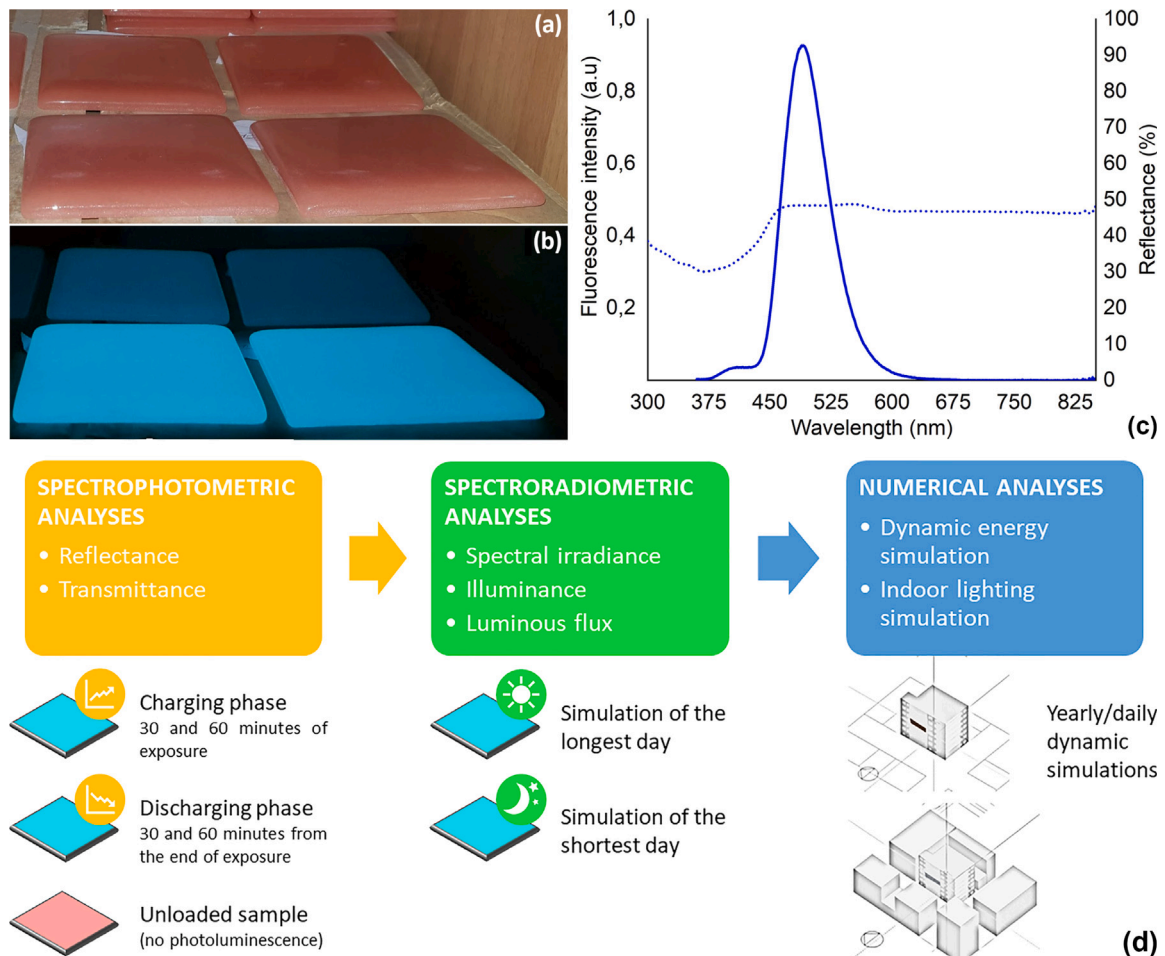


Fig. 1. Investigated tiles in their (a) inactive and (b) photoluminescent state. (c) Reflectance (dot line) and fluorescence (continuous line) spectra of the photoluminescent pigments embedded in the tiles. (d) Schematic representation of the research methodology.

blue during light emission (Fig. 1b). Fig. 1c shows reflectance and fluorescence spectra of the photoluminescent pigments embedded in the investigated tiles ($\text{Sr}_4\text{Al}_{14}\text{O}_{25}:\text{Eu}^{+2},\text{Dy}^{+3},\text{B}^{+3}$): the first is measured by means of a Varian Cary 4000 spectrophotometer, equipped with an integrating sphere, while the second is detected by an Edinburgh Instruments FS5 spectrofluorometer. Other size and color combinations are available on the market, so that a wide variety of architectural and design needs can be met. While the tested materials are small samples for the experimental characterization of optic characteristics, bigger panels can be developed for architectural integration on the external building envelope (e.g. substituting the glass of a window). The main purpose of the present research is to evaluate the potential use of photoluminescent-translucent panels as envelope elements for buildings. To this end, a two-phase methodology is followed in order to, firstly, characterize the sample from an optical and photometric point of view and, secondly, evaluate the effect of its implementation on a case-study building through numerical simulations (Fig. 1d).

3. Experimental methodology

Investigating the adaptive behavior of the sample requires an experimental characterization aimed at defining the intrinsic optical and photometric properties of the material according to different photoluminescence states. For this reason, two different investigations are performed: (i) a spectrophotometric analysis, to derive the material's optical characteristics, and (ii) a spectroradiometric analysis, aimed at evaluating the luminous contribution of the sample's afterglow, upon exposition to different irradiation conditions. As specified in

Section 1, investigations on photoluminescent materials for implementation within the built environment are at the very early stages, so that there is no standardized procedure for their characterization as building materials. For this reason, the proposed methodology makes use of acknowledged standards and techniques to define traditional materials' parameters describing the optical behavior of the sample. The main findings of the in-lab experimental campaign are then used as input parameters for the following energy and lighting numerical analyses. Indeed, since current numerical tools do not allow for the simulation of photoluminescent materials, the aforementioned optical parameters, together with photoluminescence-related photometric ones, are necessary to properly implement such materials in physical models.

3.1. Spectrophotometric characterization

A SolidSpec-3700 UV-Vis-NIR spectrophotometer is used to obtain the spectral reflectance (R%) and transmittance (T%) of the analyzed sample according to different photoluminescent states, so as to detect possible variations in the material's optical behavior. In particular, as specified in Fig. 1c, measurements are performed for: (i) the inactive case, i.e. the sample without the photoluminescent effect in progress, (ii) increasing time of exposure to the solar radiation, i.e. soon after 30 and 60 min of photoluminescence charge, (iii) increasing decay time from the end of 1-hour solicitation, i.e. respectively after 30 and 60 min of darkness. The procedure follows the ASTM E903-96 recommendations (ASTM E903-12, 2012) and three measurements of both reflectance and transmittance are performed for each case: their average values are then considered to derive the material's reflection

and transmission coefficients, using the solar spectrum irradiance provided by ASTM G173-03 (ASTM G173-03, 2020). The collected data are used to calculate the input settings for the subsequent numerical simulations. i.e., luminous and solar transmission (LT and ST) and luminous and solar reflection (LR and SR).

3.2. Spectroradiometric characterization

The photoluminescent emission of the sample is characterized by means of a specifically designed experimental campaign aimed at quantifying the emitted luminous flux under different local boundary conditions. Indeed, since the photoluminescent material is here considered as a light source, the amount of light emitted by the sample has to be characterized as a function of the incoming solar radiation throughout the year. Therefore, two scenarios are selected and used as representative limit boundary conditions of the study, i.e. the longest and the shortest day of the year. The characterization procedure consists of two subsequent tasks: first, the hourly solar irradiation hitting the sample when integrated in the specific building envelope application is calculated by means of a lighting simulation engine, secondly, the sample is exposed to the obtained solar radiation values within the controlled environment of a climatic chamber and the consequent luminous response is recorded. In the first step, the selected case-study building is modeled within the DIVA for Rhinoceros simulation environment and the photoluminescent wall is equipped with dedicated test probes for calculating the average incoming diffuse irradiation on the wall. The New York weather file is then used to correctly represent the specific climate boundary conditions. Following this preliminary analysis, an ATT DM340SR climatic chamber equipped with a BF SUN 1200 W halogen solar lamp is used to reproduce the simulated irradiation conditions and an in-lab developed integrating sphere, equipped with a JETI Specbos 1211UV spectroradiometer is used to quantify the luminous flux emitted by the photoluminescent tile upon excitation. As shown in Fig. 2, the integrating sphere is located inside the internal compartment of the climatic chamber, the sample port faces the solar lamp, while the detection port is at the same height of a lateral opening in the chamber wall, housing the spectroradiometer. Fig. 2b shows the average solar radiation values obtained from the lighting simulations on the selected portion of the building envelope, compared to the radiant flux provided by the solar simulator during the measurements in the climatic chamber. During the entire procedure, the spectroradiometer monitored both the spectral irradiance ($W/m^2 \text{ nm}$) and illuminance (lx) of the tested sample. Such data are used for: (i) the characterization of the sample itself and (ii) the calculation of the emitted luminous flux (lm) as a needed input information for the subsequent lighting simulations.

3.2.1. Luminous flux calculation

Integrating spheres are commonly used devices for the evaluation of the optical characteristics of light sources (Leloup, Leyre, Bauwens, Abeele, & Hanselaer, 2015). They consist of a Lambertian inner surface capable of homogeneously reflecting and distributing the radiation emitted by the tested lighting source. In this work, an in-lab developed integrating sphere is used to quantify the luminous flux emitted by the photoluminescent sample. The inner wall of the 43.5 cm diameter polystyrene sphere is coated with a metallic white paint, sodium chloride granules and a highly reflective barium-sulfate paint, in order to obtain a Lambertian reflecting surface. The spatial response distribution function (SRDF) of the sphere, which should be ideally constant for different angles of measurement (Ohno, 1998), is approximately flat which allows us to use the sphere for evaluating the radiant flux (ϕ) of a light source with a reasonable error. In greater detail, the relation between ϕ and the illuminance (E) detected at the exit port of the integrating sphere is given by the formula:

$$E = \frac{1}{4\pi R^2} \cdot \frac{\rho}{1-\rho} \phi \quad (1)$$

where R is the sphere's radius and ρ is the inner wall mean reflectance (Leloup et al., 2015).

4. Numerical methodology

As previously mentioned, two types of numerical analyses are carried out with different purposes: (i) yearly and daily dynamic energy simulations on the entire building and on a specifically selected area to assess the energy consumption with respect to electricity for lighting (Section 4.2) and (ii) indoor lighting simulation, focusing on the same indoor environment, to evaluate the performance of the photoluminescent-translucent panel in terms of illuminance distribution over the main surfaces (Section 4.3). The dynamic energy simulations are conducted by means of DesignBuilder software, while DIALux is exploited for lighting analyses. The following paragraphs provide more information about the case-study building and the overall procedure behind each analysis.

4.1. Case-study building

A building project located in New York City (USA) is chosen as case-study. The external envelope is, by design, a peculiar translucent envelope (Fig. 3) that allows those who look from the outside to glimpse moving shadows from within and guarantees the diffusion of natural light inside the building. Moreover, the use of photoluminescent-translucent components equips the facade with an additional luminous contribution during the hours of daylight, when it combines with the solar radiation transmitted through the translucent facade, but also during the evening, when the photoluminescent flux is the main contribution given the absence of solar radiation from the outdoors. The building contains residences for artists, offices and workshop areas, as well as exhibition spaces. Among them, a 3rd floor workshop room is selected for deeper investigations on the photoluminescent-translucent envelope behavior. The area is designed to be employed during weekdays, from 8:00 to 18:00, and its peculiar outer wall is composed as follows:

- internal glass panel (0.02 m);
- air gap (0.25 m);
- support glass (0.015 m);
- epoxy resin and glass-based photoluminescent-translucent panel, characterized by transmittance and reflectance values defined in the spectrophotometric characterization.

4.2. Dynamic energy simulations

In this work, a year-long dynamic energy simulation is conducted for investigating the lighting energy performance of the case-study building, with special focus on the electricity consumption of the selected 3rd-floor workshop area during the longest and the shortest day of the year. For the first type of analysis, both the overall and the cumulated monthly lighting consumption are taken into account. The selected case-study building is modeled using the DesignBuilder interface for EnergyPlus, which allows for the characterization of different thermal zones' occupancy profiles to properly identify their actual energy need, including the requested lighting levels for each activity during the day.

Simulations concern both yearly analyses conducted on the entire building and daily analyses focused only on the 3rd floor workshop area, during the longest and shortest day of the year (21st June and 21st December). All of them aim at comparing the effect of a non-translucent and translucent envelope on the energy performance according to different urban densities. To this purpose, three scenarios are considered: (i) the case-study building alone, with no surrounding (NS); (ii) the case-study building surrounded by a low-density context (LS); (iii) the case-study building within its actual high-rise urban environment (HS). Indeed, shading from surrounding buildings could significantly modify the results of the energy simulation, especially in terms of lighting (Bournas, 2020; Mohajeri et al., 2019).

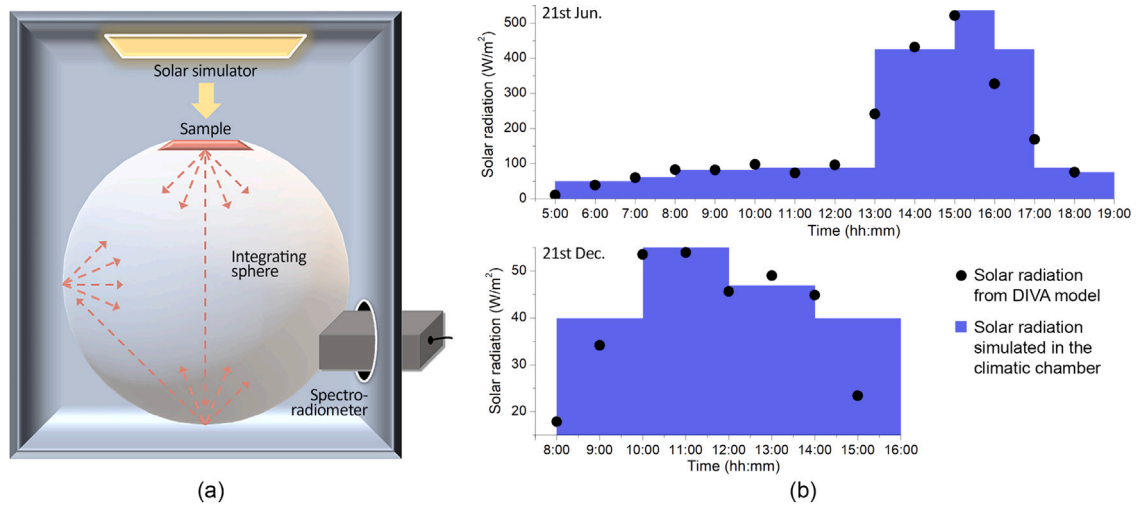


Fig. 2. (a) Experimental equipment and set up for the spectroradiometric analysis. (b) Simulated solar radiation in the climatic chamber compared with the simulated values obtained from DIVA for Rhino tool, for both the longest (21st June) and the shortest day (21st December) of the year.

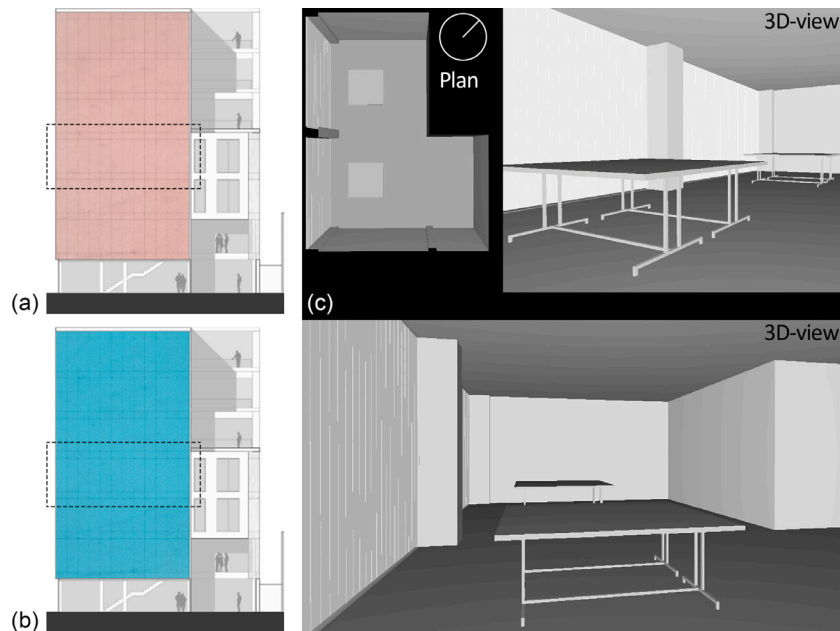


Fig. 3. Case-study building. South-West facade's translucent envelope (a) without and (b) with the photoluminescent effect in progress. (c) 3rd floor room modeled for the lighting numerical analysis (plan and 3D views).

4.2.1. Model settings and assumptions

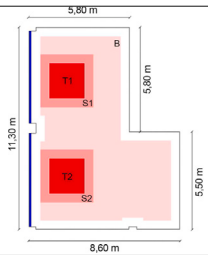
EnergyPlus daylighting model analyses daylight availability in accordance to local climate and specific site conditions as well as lighting control strategies, in response to solar gain, on a hour-by-hour basis. The input information provided to the software are: sky luminance distribution, building orientation and external obstructions (e.g. surrounding buildings), windows' size and materials' optic characteristics, directly influencing the light distribution within an indoor environment by means of wall, floor and ceiling multiple reflections. With respect to lighting control strategies, the required illuminance level is taken into account according to the activity performed in the area, as specified in the "Occupancy schedules" for each indoor area. Based on the specific model geometries and input values, the daylight factors are later calculated, i.e. the ratio between indoor illuminance to outdoor horizontal illuminance, for the specific sun-path of the simulation period and the contribution of direct light from the windows to reach the required illuminance level is evaluated. For simulating light-emitting materials,

the building envelope is modeled as purely translucent by considering the effective reflection and transmission coefficients obtained from the previously described spectrophotometric investigation, and later compared to a standard, non-translucent facade. The purely translucent and the photoluminescent-translucent configurations are supposed to have the same thermal properties and wall stratigraphy, resulting in a thermal transmittance equal to $2.63 \text{ W}/(\text{m}^2 \text{ K})$. Windows and the associated daylight entering the indoors, both from the windows and the translucent envelope, are modeled and considered for the entire building yearly simulations. Indeed, the openings are embedded in the translucent wall. The solar gains provided by the latter are, therefore, supposed to be reduced with respect to those of a standard transparent material, because of the lower coefficient of transmission characterizing the panels. The electric lighting control system is simulated to assess the energy needed to compensate the daylight illuminance level toward reaching the illuminance required in each area. For the 3rd-floor workshop room, an illuminance threshold of 300 lx at 0.80 m height is

Table 1

Illuminance and uniformity limits required by the EN 12464-1 Standard, for different areas of an office room. The plan on the right shows where these spaces are located in the considered room.

Calculation object	\bar{E}	U_0
Visual task area (T)	≥ 500 lx	≥ 0.60
Surrounding task area (S)	≥ 300 lx	≥ 0.40
Background area (B)	≥ 100 lx	≥ 0.10
Walls	≥ 50 lx	≥ 0.10
Ceiling	≥ 30 lx	≥ 0.10



assigned: this value is defined in the EN 12464-1 Standard (EN 12464-1:2011, 2011) as the minimum surrounding task area illuminance (see Section 4.3, Table 1). The satisfaction of such threshold may guarantee a highly flexible space design. Even if the focus of the work is not on consumption other than energy for lighting, the building's systems are modeled and consist in radiator heating (natural gas), boiler for hot water (electricity) and air conditioning (electricity). In the lighting simulation (Section 4.3), the 3rd-floor workshop environment openings are embedded in the photoluminescent–translucent wall, thus considering also the photoluminescent effect in addition to the translucent one.

4.3. Lighting simulations

The indoor lighting performance deals with the evaluation of the illuminance level guaranteed by the photoluminescent–translucent envelope in the selected workshop area of the case-study building. According to the EN 12464-1 Standard, a good luminous environment should satisfy three basic human needs: (i) visual comfort, which indirectly contributes to workers' productivity level; (ii) visual performance, affecting the occupants' capability of performing their visual task; (iii) visual safety. The same standard prescribes suitable values for the main parameters affecting the indoor light quality, with respect to the tasks and activities to be performed by occupants. In this framework, considering the absence of a dedicated tool to simulate photoluminescent surfaces in design software, DIALux evo (DIAL GmbH, 0000) has been chosen among the others because of the possibility to get outputs that are strictly related to the vigent standards for lighting. The selected workshop area is modeled considering its position in the building and the volume of the adjacent constructions, in order to correctly take into account, the contribution of blocking shadows. Two working tables are located in different points of the room (see Fig. 3c), for properly quantifying the illuminance parameters with respect to the specific visual task in the analysis, according to the EN 12464-1 Standard. Table 1 illustrates the target requirements in terms of illuminance values (\bar{E}) and uniformity (U_0) for the case-study lighting environment. In particular, the visual task areas (T1 and T2) are the two tables' surfaces in the room, while the surrounding task areas (S1 and S2) refer to the space around the tables and at the same height, up to 0.5 m away from their edges. Finally, the background area (B) is the remaining room's space at the ground level. Multiple simulations are performed for both the shortest and the longest day of the year, modifying the model's settings according to changes in the material's luminous emission caused, by the fluctuations in the solar radiation hitting the envelope. As previously mentioned, the final outputs were compared with the illuminance levels required by the Standard (Table 1), in order to evaluate whether the photoluminescent–translucent envelope could improve the indoor lighting quality and reduce the overall energy consumption of the building.

4.3.1. Model settings and assumptions

As previously introduced, the lighting numerical model is implemented through the DIALux software, with the aim of evaluating the luminous contribution of the photoluminescent–translucent envelope while using the experimentally measured parameters. The analytic model exploited by DIALux for lighting calculations is based on the point by point method, which allows for the illuminance level detection at a specific point (E_p) according to the following equation:

$$E_p = \frac{I_p \cdot \phi_{lamp} \cdot \cos^3 \alpha}{h^2} \quad (2)$$

where: I_p is the 1000 lumen intensity (cd) measured at the tested point; ϕ is the luminous flux (lm) of the lighting source; α is the angle between the device normal direction and the point itself; h is the distance between the lighting source and the calculation plan.

The software mainly requires three types of input data, i.e. the locational and geometrical aspects of the simulated environment, the photometric parameters of the lighting devices introduced and the optical properties of the materials involved (color, reflection and transmission coefficients). The former are necessary for the proper consideration of the building orientation, its inclusion in the surrounding urban context and the local climate: in our case, such boundary conditions are considered outside the DIALux environment, with the preliminary DIVA simulation step (Section 3.2), where the case-study building is modeled together with its surroundings and the New York weather file is implemented. Indeed, the same DIVA procedure has been used for the characterization of the amount of solar radiation hitting the photoluminescent–translucent envelope during the shortest and the longest day of the year, to lately reproduce it within the climatic chamber to detect the luminous performance of the material (Section 3.2.1). Therefore, since the obtained luminous flux data refer to the combined effect of the tile's photoluminescence and the reproduced solar radiation, DIALux simulation settings do not consider daylighting and photoluminescence separately. For this reason, no sky condition nor daylighting is added to the model, but their effect is indirectly implemented in the luminous behavior of the photoluminescent–translucent envelope. In greater detail, the latter is modeled adding multiple 10 cm-squared spotlights on the investigated surface and setting their technical features (luminous flux and correlated color temperature) according to the spectroradiometric results of the experimental analyses at different hours of day: this step is fundamental because DIALux does not allow to simulate materials that emit light, but only lighting devices. The luminous flux used as input for the 10 cm-squared lighting sources combines the diffuse radiant flux due to the incident solar radiation transmitted from the outdoor and the emitted photoluminescent radiation quantified by means of the experimental procedure described in Section 3.2.1. It is assumed that the photometric solid of the selected spotlights is representative of the way the photoluminescent tile emits and transmits light, in terms of both geometry distribution and luminous intensity. No other lighting devices are added in the model, in order to highlight just the photoluminescence-translucence luminous contribution. Finally, concerning the optical properties of the materials in the modeled environment, the investigated envelope is represented as a glass surface whose reflection and transmission coefficients come from the spectrophotometric characterization of the photoluminescent tile (Section 3.1). For the indoor ceiling, walls and floor materials, instead, standard reflection coefficients of 80%, 65% and 30% are respectively considered, following the EN 12464-1 recommendations.

5. Results from the experimental campaign

5.1. Results from the spectrophotometric analysis

In this section, the results of the in-lab spectrophotometric investigations are reported. The measured optical coefficients are employed as input parameters for the following numerical analyses. Fig. 4 represents

Table 2

Optical parameters of the investigated sample, according to different photoluminescent states: luminous/solar transmission (LT/ST) and luminous/solar reflection (LR/SR).

	Inactive case (no photol.)	30 min of exposure	60 min of exposure	30 min of decay	60 min of decay
LT (%)	16,92	11,45	12,60	11,62	11,79
ST (%)	21,96	15,65	16,65	16,42	16,13
LR (%)	11,12	11,51	11,58	11,58	11,54
SR (%)	13,80	14,39	14,55	14,53	14,42

the differences in the sample's reflectance (R%) and transmittance (T%), depending on the detected photoluminescence state. In particular, as introduced in Section 3.1, measurements are performed (i) on the inactive sample, (ii) after 30 and 60 min of exposure to solar radiation, and (iii) 30 and 60 min after the solar radiation was turned off. Following the ASTM E903-96 (ASTM E903-12, 2012) and ASTM G173-03 (ASTM G173-03, 2020) standards, reflectance and transmittance data are used to calculate reflection and transmission coefficients of the investigated sample (see Table 2).

As shown in Fig. 4 noticeable differences in both reflectance and transmittance values only occur between the inactive sample and the sample with the photoluminescent effect in progress, regardless of the charging or extinguishing phase of the phenomenon. Indeed, looking at both R% and T% profiles, it can be noticed that the offset between the curves describing the photoluminescence evolution through increasing exposure or decay times falls within the measurement's standard deviation. Therefore, it can be stated that the sample's optical behavior is not significantly altered by changes in the duration of photoluminescence charging or extinguishing period. Regarding the transition from the inactive to the light-emitting state, instead, results show how the capability of the tile to let the visible radiation pass through it (LT) is reduced by photoluminescence for about 5%, after a 30-minute exposure to solar radiation; correspondingly, the overall solar transmission (ST) decreases from 21.96% to 15.65%. On the other hand, less relevant changes can be detected among reflection coefficients' values (LR and SR) between the inactive and the emitting state.

5.2. Results from the spectroradiometric analysis

Figs. 5 and 6 show the irradiance spectra ($W/m^2 \text{ nm}$) and illuminance values (lx) of the sample, according to different intensities of the impinging solar irradiation during the two analyzed days. In particular, the emission at the maximum and minimum level of solicitation is compared to the afterglow caused only by the photoluminescent phenomenon (soon after the sunset). The corresponding colorimetric coordinates, according to the CIE 1931 XYZ color space (Smith & Guild, 1931), are also shown alongside the spectral irradiance profiles, in order to track the tile's color changes during the activation of the photoluminescent emission. Fig. 7 compares the afterglow decay in terms of illuminance (lx), as a function of time passing from the end of the tile's exposure to both the longest and the shortest day's irradiation.

The spectroradiometric analysis shows that the intensity of the exciting source strongly affects the material performance. Indeed, since the tile is a translucent material, higher solar radiation values, correspond to higher luminous fluxes in the integrating sphere. In fact, the sample's emission is given by the combination of the photoluminescent and the transmission phenomena. Soon after the sunset, i.e. at the end of the solicitation, only the photoluminescent effect remains. Indeed, both the colorimetric coordinates and the irradiance spectra of Figs. 5 and 6 show a clear difference between the cases with and without the solar radiation: the color of the sample changes from reddish to blue-green shades, while the emission spectrum narrows to a peak in the 450–550 nm wavelength range. Accordingly, also the illuminance levels guaranteed by the only photoluminescent effect are influenced

by the intensity of previous solicitation. Fig. 7 shows the trend of the afterglow decay during the first hour after the exposure of the sample to solar radiation: the values of illuminance of the longest day of the year are always higher than those related to the shortest, even if the lighting contribution fades rather quickly in both the cases.

6. Results from the numerical analyses

6.1. Dynamic energy performance

The results from the dynamic energy simulations are reported below. In Fig. 8, the electricity consumption for lighting of the entire building is showed according to different urban scenarios (NS, LS and HS): the influence of the translucent envelope is compared to that of a standard non-translucent one. Light passing throughout the envelope is the only difference between the translucent and non-translucent simulations, thus the other thermal characteristics are the same. Accordingly, Tables 3 and 4 quantify the same comparison in terms of lighting electricity consumption and saving, respectively. Considering the NS scenario, the translucent envelope guarantees almost a 40% electricity saving for lighting throughout the year, and up to a 58% consumption reduction during the most-luminous month, i.e. June. LS and HS scenarios, instead, allow lower yearly savings (about -38.43% and -25.52% respectively), compared to the application of a non-translucent envelope. As expected, these reductions in energy for lighting are particularly high from April to September, when daylight duration is longer. Moreover, the actual scenario (HS) implies the lowest savings due to the light-blocking effect of surrounding buildings. Fig. 9 summarizes the effect of the translucent envelope for different urban surroundings in terms of lighting energy demand (kWh).

Moving from the entire building to the selected 3rd-floor workshop area, Tables 5 and 6 respectively report the lighting electricity consumption and saving during the shortest (21st December) and the longest day (21st June) of the year, always comparing NS, LS and HS scenarios. A sensible difference is obviously detected between the two days because of daylight duration: savings are up to -28.1% for the shortest day (0.21 kW/m^2 instead than 0.29 kW/m^2), and up to -76.7% for the longest day (0.07 kWh/m^2 instead than 0.29 kWh/m^2), with respect to the non-translucent envelope. While the contribution of lighting passing through the translucent envelope lasts the entire room usage-time (8:00–19:00) for the longest day, it stops at 17:00 for the shortest one (Fig. 10). The greater positive contributions of natural daylight from the translucent envelope are: (i) during mid-morning, from 10:00 to 11:00 of 21st December, when it is possible to save up to 47.9% of energy, and (ii) during the afternoon, from 15:00 to 19:00 of 21st June, when up to 90% of electricity can be saved. These results are due to the exposition and orientation of the considered indoor area, which is west-facing and located at the 3rd floor: while in NS and LS cases almost no-obstructions shade the considered room, in the actual HS condition a high building prevents sunlight from reaching the facade. As previously specified, these analyses allow to assess the electricity savings due to the only translucent behavior of the facade: the additional photoluminescence contribution is not accounted in the dynamic yearly and daily simulations. The following sections focus on the latter, reporting the main findings in terms of lighting numerical performance.

6.2. Lighting performance

In this section, results from lighting simulations on the selected 3rd-floor area (HS scenario) are reported with respect to maintained illuminance (\bar{E}) and uniformity (U_0) calculated on (i) the main room surfaces (ceiling and walls) and (ii) visual task areas. In particular, the latter involve not only the space where the task takes place, i.e. the two working tables in the room, but also the related surrounding areas (at

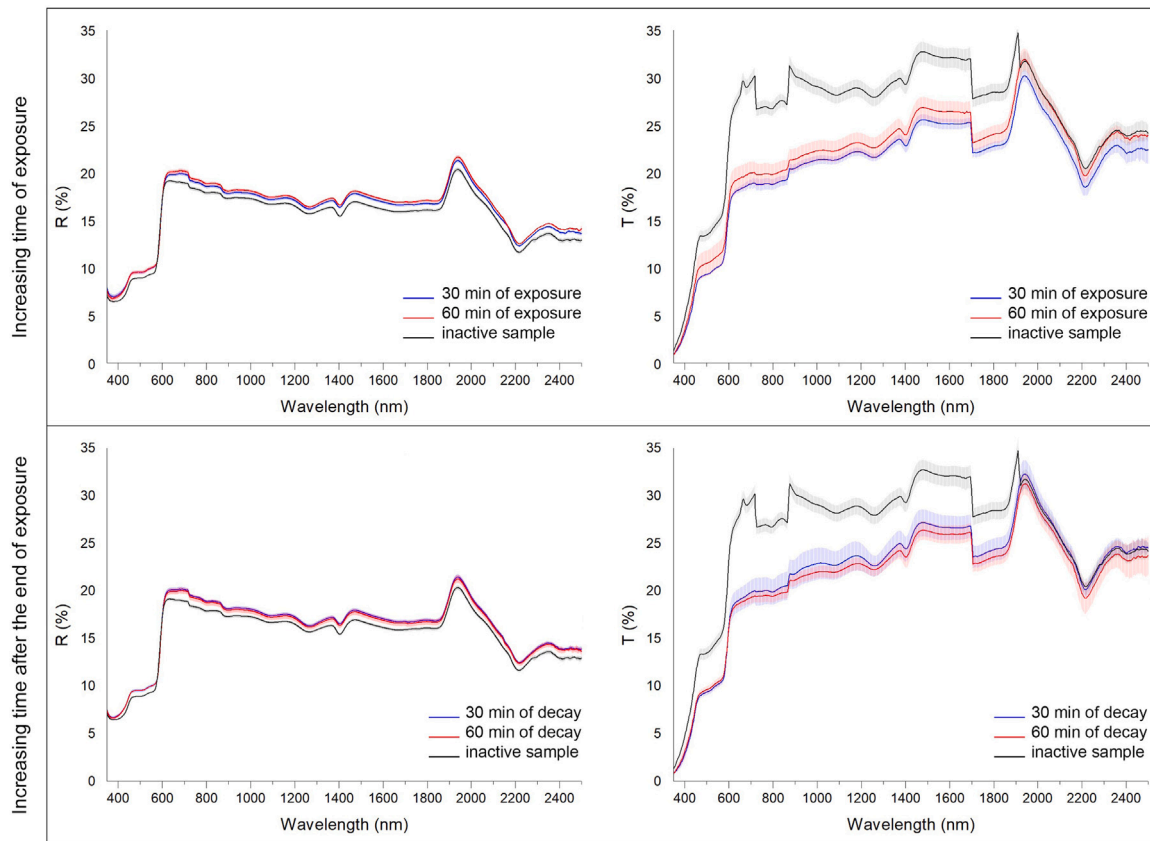


Fig. 4. Reflectance (R%) and transmittance (T%) profiles of the investigated sample, according to its inactive state and both charging and discharging photoluminescence phases.

Table 3

Electricity consumption for lighting (kWh/m²) considering the entire building in different urban densities: comparison between translucent (T) and non-translucent envelope.

Month	T-NS	NS	T-LS	LS	T-HS	HS
January	1.46	1.87	1.51	1.92	1.67	1.92
February	1.19	1.68	1.25	1.74	1.42	1.74
March	1.16	1.87	1.24	1.96	1.49	1.96
April	0.89	1.71	0.98	1.80	1.25	1.80
May	0.88	1.86	0.98	1.96	1.30	1.96
June	0.75	1.78	0.86	1.89	1.16	1.89
July	0.77	1.77	0.87	1.87	1.17	1.87
August	0.84	1.85	0.95	1.96	1.28	1.96
September	0.97	1.75	1.05	1.84	1.32	1.84
October	1.21	1.84	1.28	1.92	1.52	1.92
November	1.41	1.84	1.46	1.89	1.62	1.89
December	1.46	1.83	1.50	1.87	1.64	1.87

the same height of the tables) and the whole background environment (at the ground level).

Tables 7 and 8 give an overview on the diurnal indoor visual environment guaranteed by the daylight passing through translucent envelope, respectively during the shortest and the longest day of the year. No other artificial lighting devices are considered, in order to see if the translucence alone could avoid further electrical consumption and costs. On the other hand, Table 9 focuses on lighting provided by the only photoluminescence, i.e. in the absence of external solar radiation. As described in Section 4.3.1, the photoluminescent sample is modeled as a spotlight device with the same photometric properties obtained from the experimental campaign. However, a minimum luminous flux (ϕ) of 1 lumen is required in the simulation engine for each luminaire, which is higher than the sample's average emission intensity

Table 4

Electricity saving for lighting (%) considering the entire building in different urban densities, with respect to the non-translucent envelope (on the left) and to the actual HS scenario (on the right).

Month	T-NS	T-LS	T-HS	NS	LS	HS
January	-22.0	-21.1	-13.1	-12.5	-9.2	Ref
February	-29.2	-28.4	-18.0	-16.6	-12.6	Ref
March	-38.2	-36.9	-24.2	-22.2	-16.7	Ref
April	-47.8	-45.4	-30.3	-28.8	-21.6	Ref
May	-52.5	-49.9	-33.9	-32.1	-24.2	Ref
June	-57.6	-54.6	-38.3	-35.3	-26.4	Ref
July	-56.5	-53.6	-37.5	-34.2	-25.8	Ref
August	-54.6	-51.8	-34.7	-34.6	-26.2	Ref
September	-44.7	-43.0	-28.3	-26.6	-20.6	Ref
October	-34.2	-33.1	-21.0	-20.0	-15.4	Ref
November	-23.1	-22.6	-14.0	-13.0	-10.0	Ref
December	-20.1	-19.8	-12.2	-11.0	-8.6	Ref
Year	-39.9	-38.4	-25.5	-22.9	-17.3	Ref

(see Fig. 7). Therefore, Table 9 provides a parametric analysis of the envelope potential, hypothesizing the material to guarantee higher ϕ values toward the satisfaction of the EN 12464-1 requirements. Results reported for every item of Tables 7–9 correspond to the minimum illuminance values reached on the elements of each specific category. The check symbols near the numerical values indicate whether the Standard recommendations are met or not.

Simulations outputs show that the lighting distributions always have a proper uniformity (U_0), while the required illuminance levels are never contemporaneously reached for all room's surfaces. In particular, during the daylight hours of the shortest day of the year (Table 7), the here-proposed photoluminescent-translucent envelope guarantees a sufficient illuminance on the ceiling of the room (46.1 lx), while all the

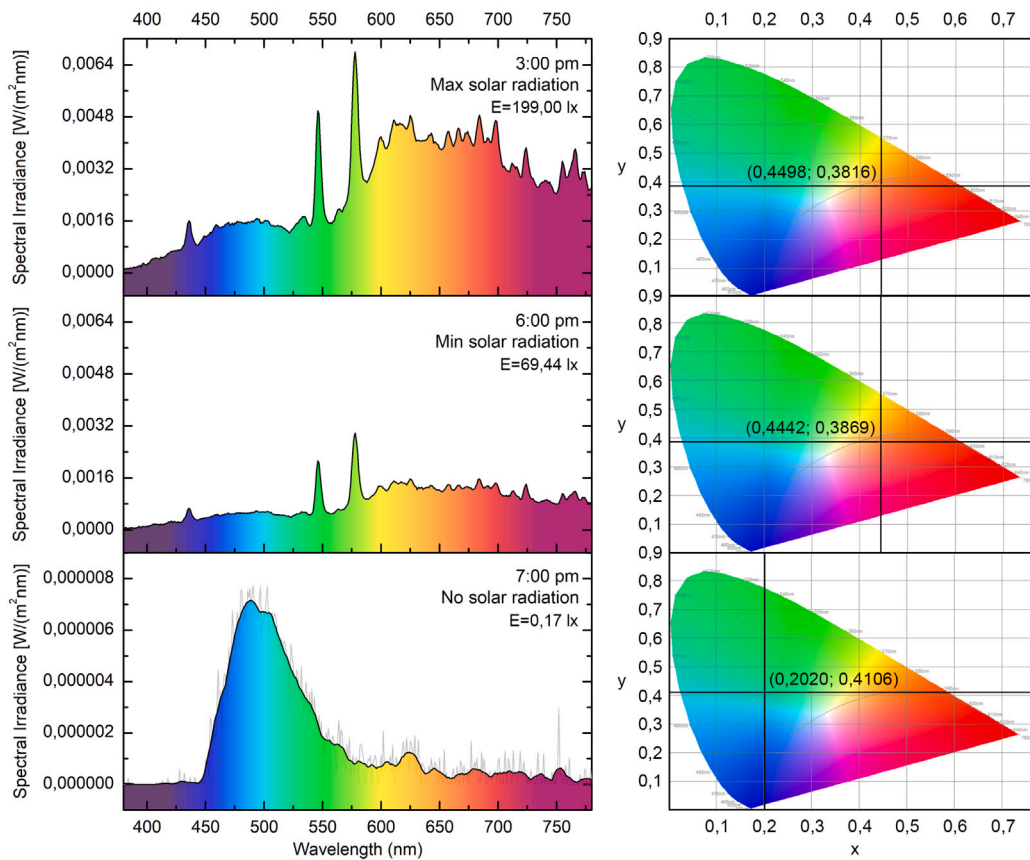


Fig. 5. Spectral irradiance of the photoluminescent sample (on the left) and correlated colorimetric coordinates (on the right), during the extreme solar radiation conditions of the longest day of the year. (For interpretation of the references to color in this figure legend, the reader is referred to the web version of this article.)

Table 5

Electricity consumption for lighting (kW) during the longest and the shortest day of the year, considering the selected 3rd-floor area and different urban densities: comparison between translucent (T) and non-translucent envelope.

Time	21st December			21st June			Ref
	T-NS	T-LS	T-HS	T-NS	T-LS	T-HS	
8:00	1.76	1.77	1.88	1.22	1.26	1.72	1.92
9:00	1.16	1.22	1.61	0.70	0.77	1.54	1.92
10:00	0.90	1.02	1.45	0.34	0.45	1.26	1.92
11:00	1.00	1.14	1.61	0.46	0.60	1.30	1.92
12:00	1.06	1.17	1.68	0.49	0.66	1.41	1.92
13:00	1.17	1.24	1.68	0.75	0.93	1.57	1.92
14:00	1.07	1.13	1.67	0.45	0.63	1.38	1.92
15:00	1.08	1.13	1.71	0.19	0.19	0.80	1.92
16:00	1.62	1.64	1.84	0.19	0.19	0.24	1.92
17:00	1.92	1.92	1.92	0.19	0.19	0.19	1.92
18:00	1.92	1.92	1.92	0.19	0.19	0.19	1.92
19:00	1.92	1.92	1.92	0.19	0.19	0.19	1.92
Day [kW]	16.60	17.22	20.89	5.37	6.27	11.79	23.09
Day [kW/m ²]	0.21	0.22	0.26	0.07	0.08	0.15	0.29

other surfaces do not reach the minimum threshold. Better results are found in the longest day of the year (Table 8), when the lighting level of the main room surfaces (walls, ceiling and background) fulfills the Standard request during almost the whole working day, i.e. from 10:00 am to 6:00 pm. In this period, the minimum illuminance value on the punctual visual task areas (500 lx) is still not reached, but it would be easily compensated by the addition – for instance – of proper lamps on the desks. As previously mentioned, the evaluation of the only photoluminescence contribution in the indoor lighting environment, i.e. without

Table 6

Electricity saving for lighting (%) during the longest and the shortest day of the year, considering the selected 3rd-floor area and different urban densities, with respect to the non-translucent envelope.

Time	21st December			21st June		
	NS	LS	HS	NS	LS	HS
8:00	-8.6	-8.1	-2.3	-36.4	-34.4	-10.7
9:00	-39.6	-36.6	-16.3	-63.6	-59.7	-20.0
10:00	-53.1	-47.2	-24.8	-82.5	-76.5	-34.5
11:00	-47.9	-41.0	-16.5	-75.9	-69.0	-32.3
12:00	-44.7	-39.0	-12.8	-74.6	-65.9	-26.7
13:00	-39.0	-35.8	-12.6	-61.2	-51.4	-18.5
14:00	-44.3	-41.1	-13.3	-76.7	-67.0	-28.4
15:00	-43.9	-41.5	-11.0	-90.0	-90.0	-58.5
16:00	-15.9	-14.9	-4.6	-90.0	-90.0	-87.5
17:00	0.0	0.0	0.0	-90.0	-90.0	-90.0
18:00	0.0	0.0	0.0	-90.0	-90.0	-90.0
19:00	0.0	0.0	0.0	-90.0	-90.0	-90.0
Day	-28.1	-25.4	-9.5	-76.7	-72.8	-48.9

the solar radiation passing through the photoluminescent-translucent envelope, is proposed as a parametric study aimed at improving the material’s performance. For demonstrative purposes, the hypothetical luminous flux emitted by the single photoluminescent tile was gradually increased until the lighting contribution of the entire envelope satisfied the lighting requirements, at least for the main surfaces of the room (ceiling, walls and background). To this end, the parametric study demonstrated that a final value of 20 lumen has proven to be sufficient to this aim.

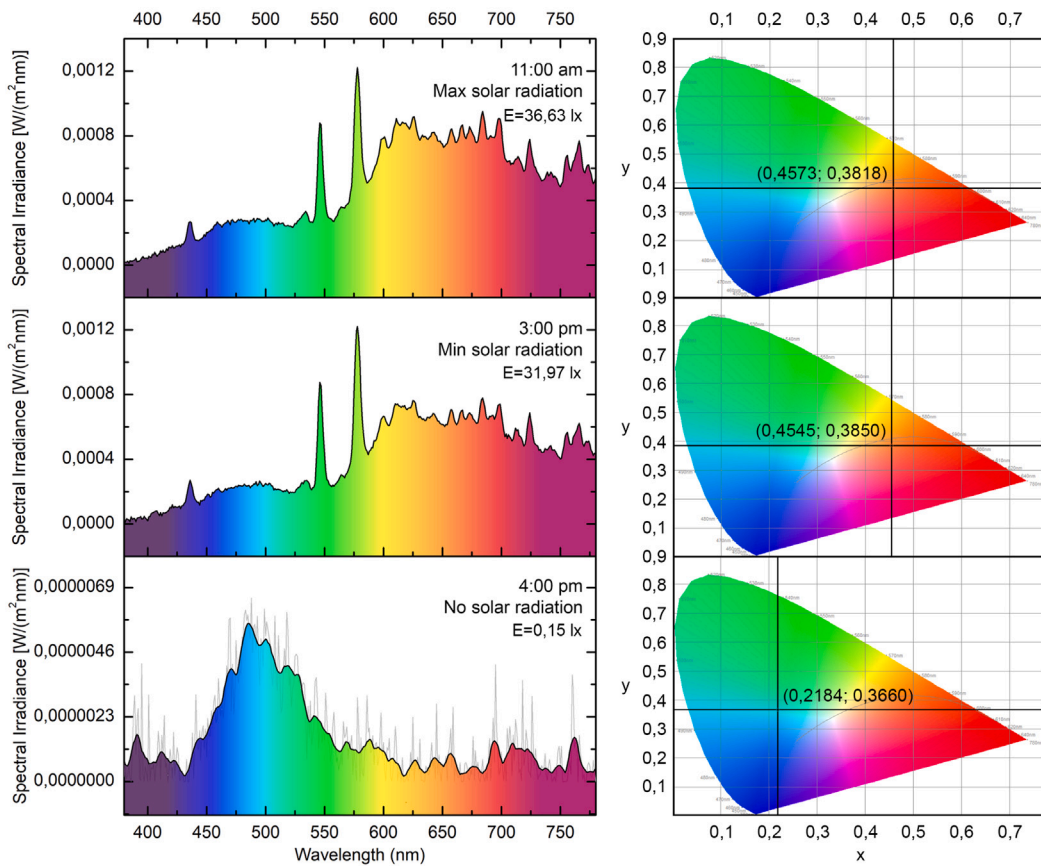


Fig. 6. Spectral irradiance of the photoluminescent sample (on the left) and correlated colorimetric coordinates (on the right), during the extreme solar radiation conditions of the shortest day of the year. (For interpretation of the references to color in this figure legend, the reader is referred to the web version of this article.)

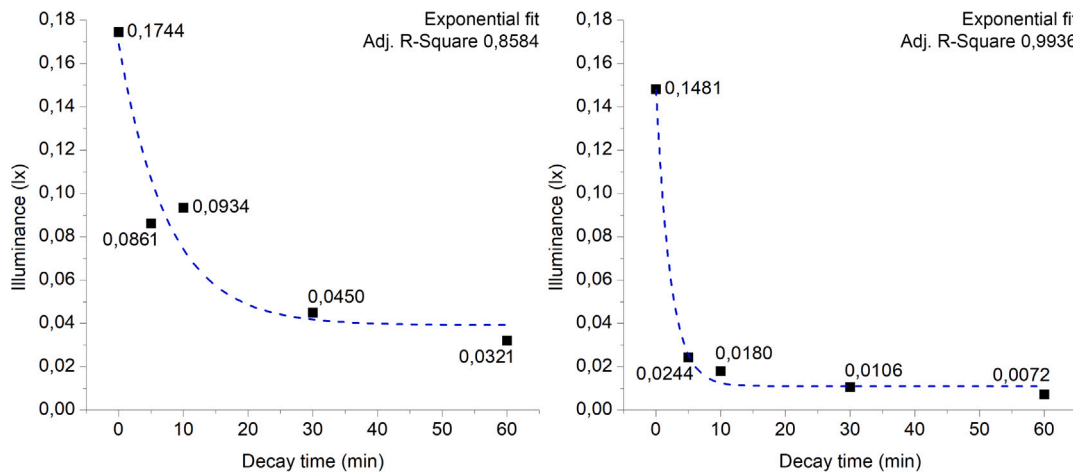


Fig. 7. Afterglow decay in terms of illuminance (lx), during the first hour after the end of the solicitation. Longest (on the left) and shortest (on the right) day of the year.

7. Discussions over the obtained results

The experimental and numerical analyses performed on the selected photoluminescent–translucent tiles highlight the peculiarity of the material as possible light-emitting building component. Indeed, its capacity of transmitting daylight (21.96%) if applied as building envelope material is lowered (around 15%–16%) by the activation of the photoluminescent state in the dark, resulting in a contribution in terms of indoor illuminance that directly depends on the diurnal

solar irradiation power. However, despite the promising potential, the need for both materials’ optimization and proper characterization procedures is evident. The first comes from the low lighting intensity provided by the material since the very beginning of the afterglow decay (0.17 lx, after the longest day of the year), while the second moves from the need to take into account the real exposure conditions that affect the photoluminescence performance. In addition, no dedicated lighting tools currently exist capable of modeling light-emitting materials, which indeed severely hinders their consideration for urban

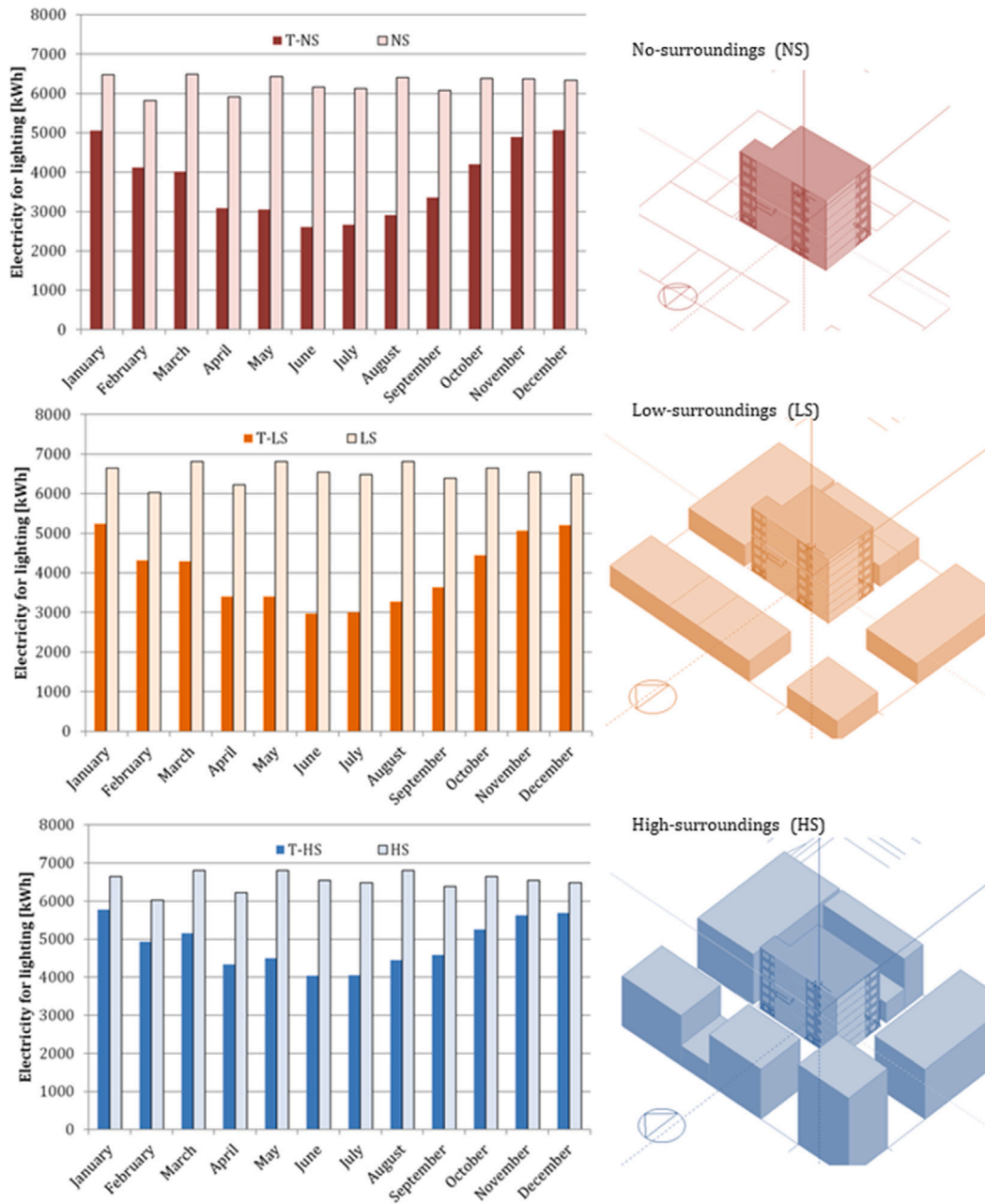


Fig. 8. Yearly energy performance for lighting, considering the entire building in different urban densities: comparison between translucent (T) and non-translucent envelope.

solutions. Similar issues were detected by other studies on different types of photoluminescent materials (Chiatti, Fabiani, Cotana et al., 2021; Fabiani et al., 2021), leading to assumptions and simplifications for the execution of statistical and numerical analyzes.

With respect to the entire-building lighting energy simulations, the following considerations can be made on the role of the translucent envelope: (i) it is effective in significantly lowering the yearly energy for lighting (up to 40%) with respect to the corresponding non-translucent case; (ii) when considering seasonal behavior, savings are higher in July, i.e. the most luminous month, where the translucent envelope is able to save up to 58% energy for lighting with respect to the corresponding non-translucent envelope; (iii) yearly savings are higher for no-surroundings (NS) (up to 40%), while low-surroundings (LS) and high-surroundings (HS) scenarios entail lower savings (38% and 25%, respectively) with respect to the corresponding non-translucent envelope. Focusing on the lighting energy simulation for the specific west-faced, 3rd floor workshop room, instead, the main findings can

be synthesized as follows: (i) considering daily lighting performance, during the shortest day of the year (21st December), electricity for lighting is reduced up to 28% due to the translucent envelope, while during the longest day of the year (21st June), savings are much higher, up to 77%; (ii) savings are higher during mid-morning (10:00–11:00) for the shortest day, while the higher savings for the longest day are in the afternoon-evening (15:00–19:00), due to different sun duration depending on the season. Finally, hypothesizing an emitted luminous flux of 1 lm for each tile composing the photoluminescent-translucent envelope, 6.8–10.4 lux could be provided in the background and surrounding task area of the investigated workshop room. Considering also the photoluminescence afterglow duration (Fig. 7), the peculiar facade could manage, alone, to further contribute almost 5% reduction in electricity consumption with respect to the only translucent one (daily value for the 21st June). This percentage is valid for the daily analysis of the longest day, where the calculated contribution (from the lighting performance section) is added to the needed illuminance

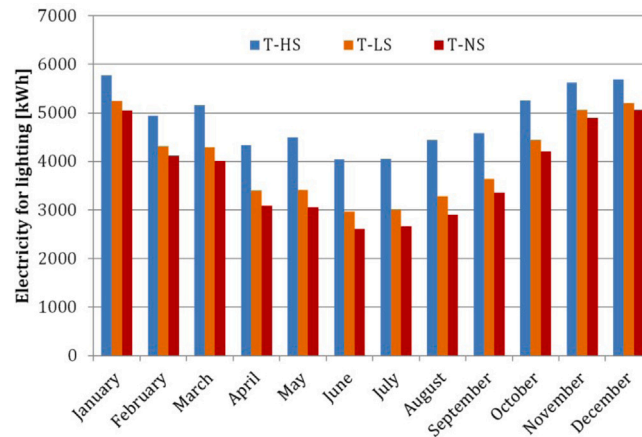


Fig. 9. Yearly energy performance for lighting, considering the entire building with the translucent envelope (T) in different urban densities.

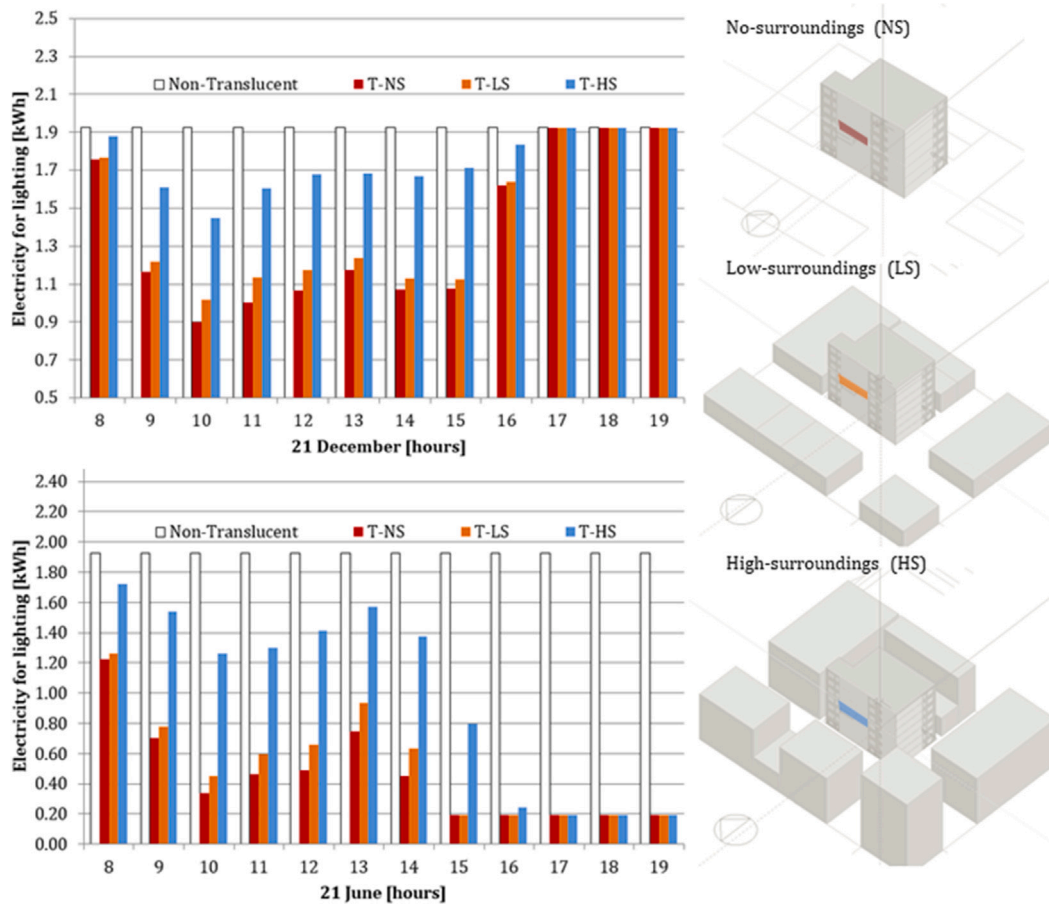


Fig. 10. Daily energy performance for lighting, considering the selected 3rd-floor area and different urban densities: comparison between translucent (T) and non-translucent envelope.

of the dynamic performance. It should be specified that the photoluminescent contribution to lighting is provided regardless the surrounding environment (NS, LS or HS), as the material is able to “charge” also with cloudy and shadowy surrounding condition and its performance is not modified by it (see Fig. 11).

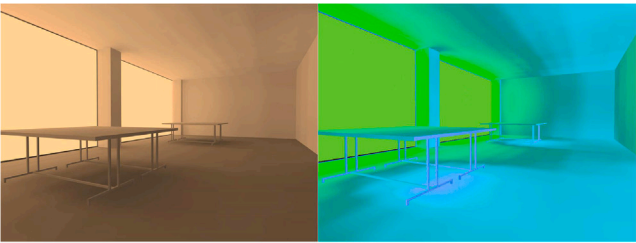
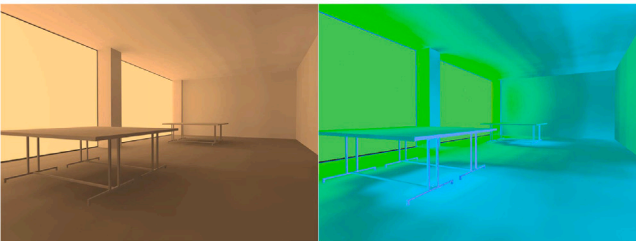
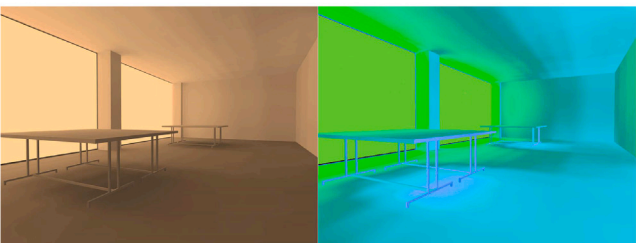
8. Conclusions

In this article, innovative photoluminescent–translucent materials for building envelope application are studied. Their advanced dynamic performance is investigated by means of a coupled experimental–numerical method. Final results reply to the posited research questions

(Section 1.1). photoluminescent–translucent envelope materials contribute in reducing electricity consumption for lighting in buildings, when they are employed as facades’ components. Considering a case-study building in New York City (USA), a yearly lighting electricity demand reduction of up to 40% can be provided by the only translucent property of the material, with respect to the standard non-translucent envelope. On a daily basis and focusing on a specific 3rd-floor indoor area of the same building, instead, the translucent envelope is able to reduce up to 28% the electricity consumption during the shortest day of the year (21st December) and up to 77% during the longest day of the year (21st June). The contribution of photoluminescence allows to

Table 7

Results from DIALux simulations during the daylight hours of the shortest day of the year. Figures show the rendering view (on the left) and the false color image (on the right) of the simulated room.

Time (hh:mm) / Single tile luminous flux (ϕ)	Object	\bar{E}	U_0
From 8:00 to 10:00 / $\phi = 7$ lm			
	Ceiling	46.1 lx	✓ 0.39
	Walls	21.1 lx	× 0.59
	Task area	69.9 lx	× 0.77
	Surrounding area	73.0 lx	× 0.63
	Background area	47.3 lx	× 0.49
From 10:00 to 12:00 / $\phi = 8$ lm			
	Ceiling	52.7 lx	✓ 0.39
	Walls	24.1 lx	× 0.59
	Task area	79.8 lx	× 0.77
	Surrounding area	83.4 lx	× 0.63
	Background area	54.0 lx	× 0.49
From 12:00 to 16:00 / $\phi = 7$ lm			
	Ceiling	46.1 lx	✓ 0.39
	Walls	21.1 lx	× 0.59
	Task area	69.9 lx	× 0.77
	Surrounding area	73.0 lx	× 0.63
	Background area	47.3 lx	× 0.49

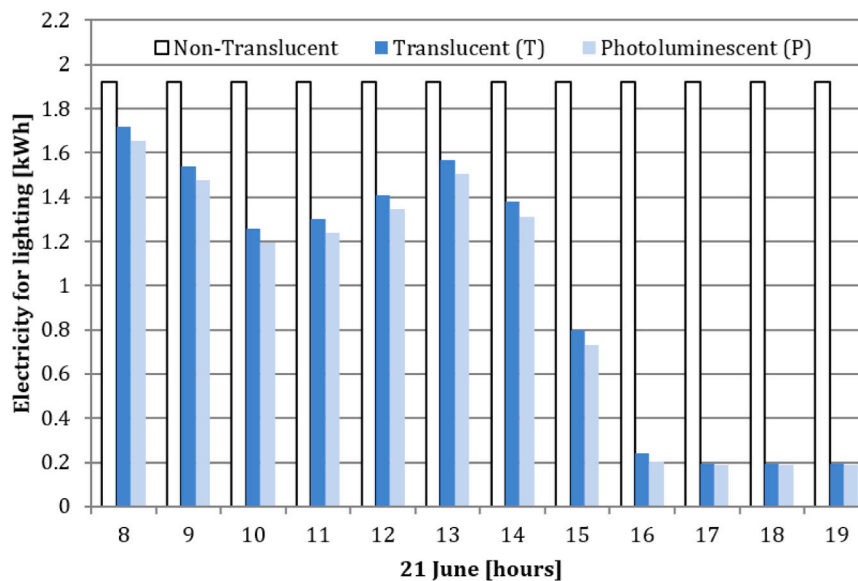
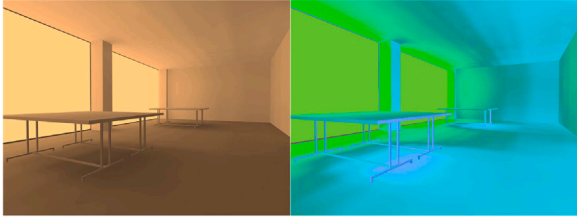
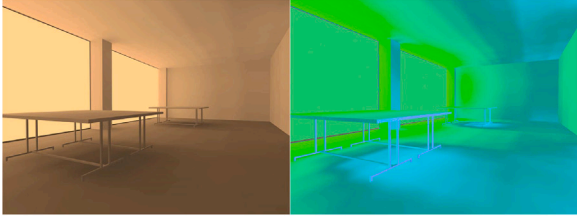
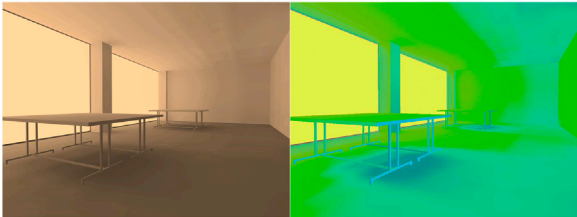
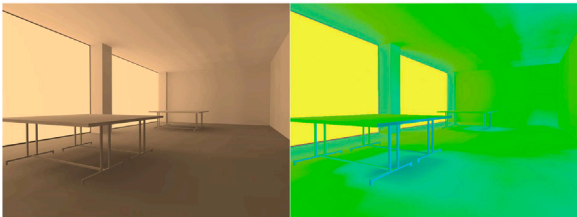


Fig. 11. Daily energy performance of the considered indoor area in the case-study building, with respect to electricity for lighting: comparison between the non-translucent, translucent and photoluminescent-translucent envelope. The numerical analysis is conducted with respect to the HS scenario, but the contribution of photoluminescence is the same for all the cases.

Table 8

Results from DIALux simulations during the daylight hours of the longest day of the year. Figures show the rendering view (on the left) and the false color image (on the right) of the simulated room.

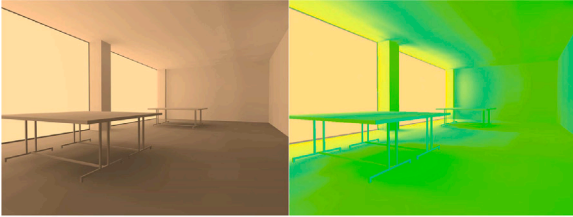
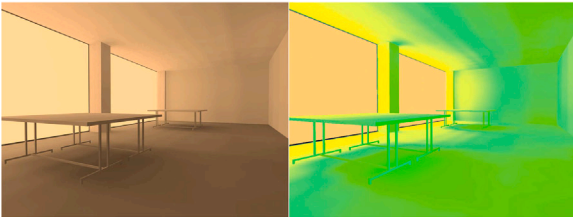
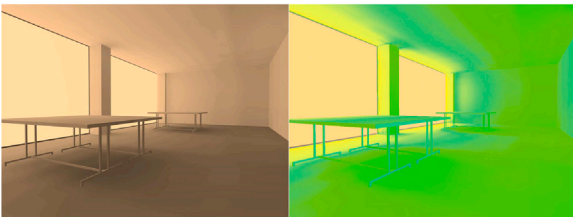
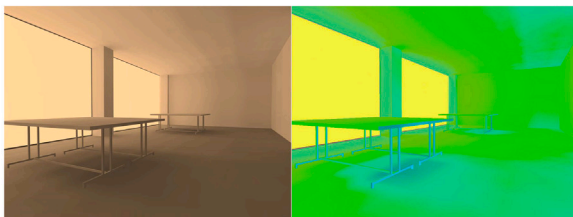
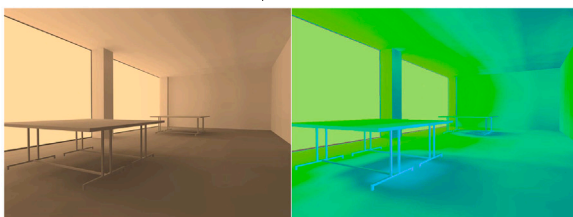
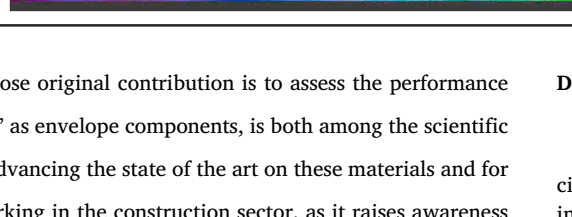
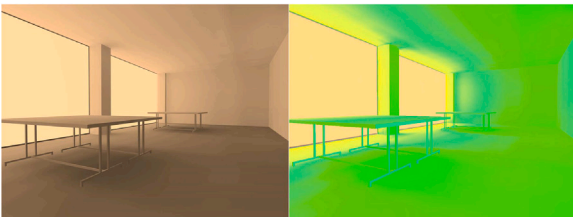
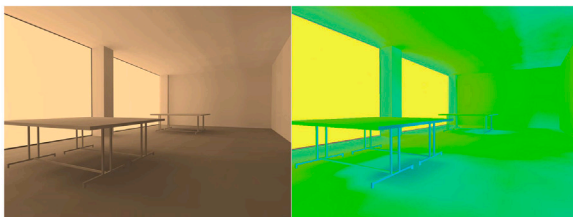
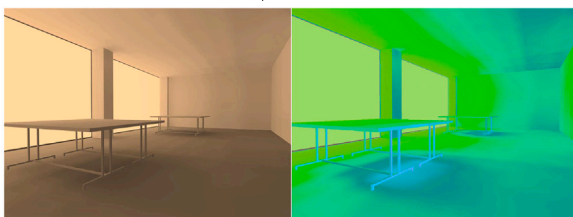
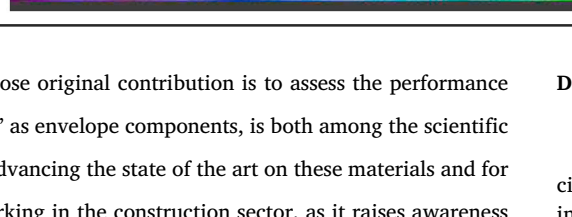
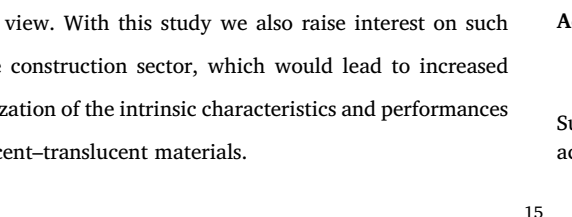
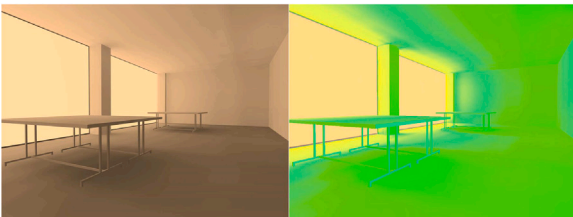
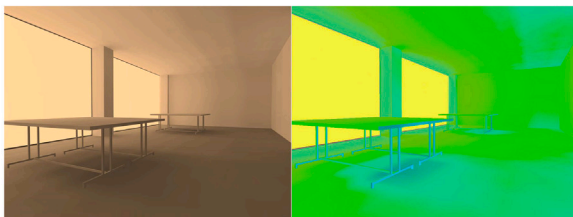
Time (hh:mm) / Single tile luminous flux (ϕ)	Object	\bar{E}	U_0
From 5:00 to 7:00 / $\phi = 7$ lm			
	Ceiling	46.1 lx	✓ 0.39
	Walls	21.1 lx	× 0.59
	Task area	69.9 lx	× 0.77
	Surrounding area	73.0 lx	× 0.63
	Background area	47.3 lx	× 0.49
From 7:00 to 8:00 / $\phi = 9$ lm			
	Ceiling	59.3 lx	✓ 0.39
	Walls	27.1 lx	× 0.59
	Task area	89.9 lx	× 0.76
	Surrounding area	93.7 lx	× 0.63
	Background area	60.7 lx	× 0.50
From 8:00 to 10:00 / $\phi = 15$ lm			
	Ceiling	98.9 lx	✓ 0.39
	Walls	45.2 lx	× 0.59
	Task area	150 lx	× 0.78
	Surrounding area	156 lx	× 0.63
	Background area	101 lx	✓ 0.49
From 10:00 to 13:00 / $\phi = 18$ lm			
	Ceiling	119 lx	✓ 0.39
	Walls	54.2 lx	✓ 0.59
	Task area	180 lx	× 0.76
	Surrounding area	187 lx	× 0.63
	Background area	121 lx	✓ 0.50
From 13:00 to 15:00 / $\phi = 34$ lm			

(continued on next page)

add 5% reductions to the daily saving assessed for the 21st June for the translucent case. The surrounding urban environment influences the amount of energy saving, by preventing solar radiation to reach the envelope of the considered building. While the absence of near constructions (NS) guarantees the optimal saving values, low surroundings (LS) and high surroundings (HS) show yearly 5.6% and 22.9% increase in consumption, respectively. On the other hand, the reduction of daylight hitting the envelope caused by the surroundings' shading effect does not modify the contribution of photoluminescence, which is unchanged for NS, LS, HS scenarios, as the materials are charged even by diffuse conditions. The illuminance and uniformity guaranteed by the translucent behavior of the envelope are confirmed by the daily lighting simulations, which also assess the punctual contribution of photoluminescence. A further optimization of the photoluminescent-translucent materials in terms of emitted luminous flux could allow for a more significant and durable contribution to lighting. As it currently

is, they show a fast afterglow decay from the end of the exposure to the activating luminous source that also need to be improved for possible implementation in the lighting sector. The emitted light is colored in the case of the considered blue-to-lobster-red samples, thus this application could have interesting architectural features for applications in peculiar indoor areas, such as exhibitions. However, the afterglow color can be chosen also to be almost white, guaranteeing suitable indoor light color also for offices of residential functions. Concluding, the investigated materials represent a promising solution for the constructions sector, both for architectural expression-variety as well as energy saving purpose, to expand the current library of gray solutions toward Urban Heat Island mitigation and cooling cities. Indeed, such materials could potentially be integrated in the external envelope of the building, such as in double-glass solutions for windows, providing innovative architectural expression and characterizing not only the indoors but also the outdoor urban environment. The relevance

Table 8 (continued).

	Ceiling	224 lx	✓	0.39
	Walls	102 lx	✓	0.60
<p>From 15:00 to 16:00 / $\phi = 44$ lm</p> 	Task area	340 lx	×	0.77
	Surrounding area	354 lx	✓	0.64
<p>From 16:00 to 17:00 / $\phi = 34$ lm</p> 	Background area	229 lx	✓	0.48
	Ceiling	224 lx	✓	0.39
<p>From 17:00 to 18:00 / $\phi = 18$ lm</p> 	Walls	102 lx	✓	0.60
	Task area	340 lx	×	0.77
<p>From 18:00 to 19:00 / $\phi = 12$ lm</p> 	Surrounding area	354 lx	✓	0.64
	Background area	229 lx	✓	0.48
	Ceiling	290 lx	✓	0.39
	Walls	132 lx	✓	0.60
<p>From 16:00 to 17:00 / $\phi = 34$ lm</p> 	Task area	439 lx	×	0.77
	Surrounding area	458 lx	✓	0.64
<p>From 17:00 to 18:00 / $\phi = 18$ lm</p> 	Background area	297 lx	✓	0.48
	Ceiling	119 lx	✓	0.39
<p>From 18:00 to 19:00 / $\phi = 12$ lm</p> 	Walls	54.2 lx	✓	0.59
	Task area	180 lx	×	0.76
	Surrounding area	187 lx	×	0.63
	Background area	121 lx	✓	0.50
	Ceiling	79.1 lx	✓	0.39
	Walls	36.1 lx	×	0.59
<p>From 16:00 to 17:00 / $\phi = 34$ lm</p> 	Task area	120 lx	×	0.77
	Surrounding area	125 lx	×	0.63
<p>From 17:00 to 18:00 / $\phi = 18$ lm</p> 	Background area	81 lx	✓	0.48



of this study, whose original contribution is to assess the performance of such materials' as envelope components, is both among the scientific community for advancing the state of the art on these materials and for professionals working in the construction sector, as it raises awareness on a material that could benefit buildings from the energy and architectural point of view. With this study we also raise interest on such materials for the construction sector, which would lead to increased usage and optimization of the intrinsic characteristics and performances of photoluminescent-translucent materials.

Declaration of competing interest

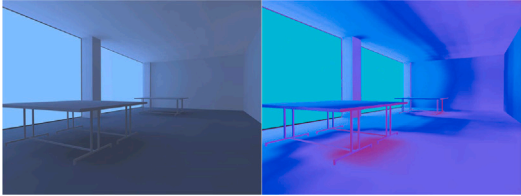
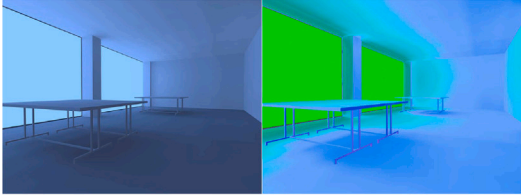
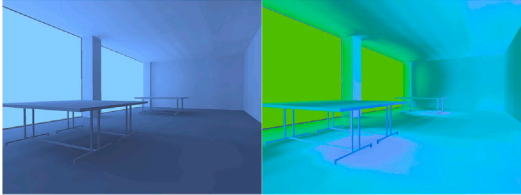
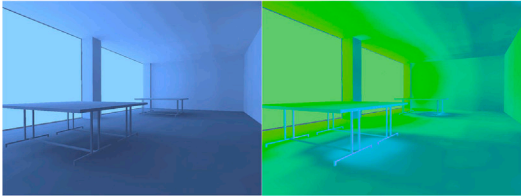
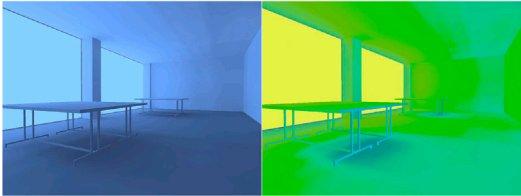
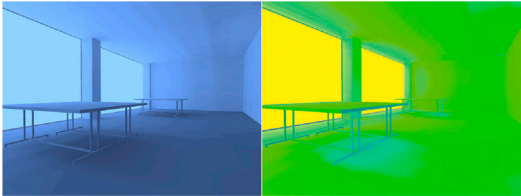
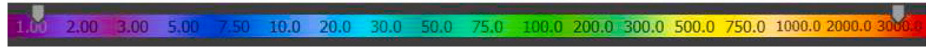
The authors declare that they have no known competing financial interests or personal relationships that could have appeared to influence the work reported in this paper.

Acknowledgments

C.C.'s acknowledgments are due to the PhD school in Energy and Sustainable Development from University of Perugia. F.R. gratefully acknowledges Ermenegildo Zegna Founder's Scholarship 2019–2020.

Table 9

Results from DIALux simulations concerning the photoluminescent contribution of the envelope, according to different hypothesis on the material's performance. Figures show the rendering view (on the left) and the false color image (on the right) of the simulated room.

Hypothetical luminous flux (ϕ)	Object	\bar{E}	U_0
$\phi = 1 \text{ lm}$			
	Ceiling	6.59 lx	× 0.39
	Walls	3.01 lx	× 0.59
	Task area	9.97 lx	× 0.77
	Surrounding area	10.4 lx	× 0.63
	Background area	6.75 lx	× 0.49
$\phi = 3 \text{ lm}$			
	Ceiling	19.8 lx	× 0.39
	Walls	9.03 lx	× 0.59
	Task area	30.0 lx	× 0.77
	Surrounding area	31.2 lx	× 0.63
	Background area	20.2 lx	× 0.48
$\phi = 5 \text{ lm}$			
	Ceiling	32.9 lx	✓ 0.39
	Walls	15.1 lx	× 0.59
	Task area	50.0 lx	× 0.77
	Surrounding area	52.0 lx	× 0.63
	Background area	33.7 lx	× 0.48
$\phi = 10 \text{ lm}$			
	Ceiling	65.9 lx	✓ 0.39
	Walls	30.1 lx	× 0.59
	Task area	100 lx	× 0.77
	Surrounding area	104 lx	× 0.63
	Background area	67.4 lx	× 0.48
$\phi = 15 \text{ lm}$			
	Ceiling	98.9 lx	✓ 0.39
	Walls	45.2 lx	× 0.59
	Task area	150 lx	× 0.78
	Surrounding area	156 lx	× 0.63
	Background area	101 lx	✓ 0.48
$\phi = 20 \text{ lm}$			
	Ceiling	132 lx	✓ 0.39
	Walls	60.2 lx	✓ 0.59
	Task area	200 lx	× 0.77
	Surrounding area	208 lx	× 0.63
	Background area	135 lx	✓ 0.48
			

References

- Ahuja, A., & Mosalam, K. (2017). Evaluating energy consumption saving from translucent concrete building envelope. *Energy and Buildings*, 153, 448–460. <http://dx.doi.org/10.1016/j.enbuild.2017.06.062>.
- A. E903-12 (2012). *Standard test method for solar absorptance, reflectance, and transmittance of materials using integrating spheres: Tech. rep.*, West Conshohocken, PA: ASTM International, <http://dx.doi.org/10.1520/E0903-12>.
- A. G173-03 (2020). *Standard tables for reference solar spectral irradiances: Direct normal and hemispherical on 37° tilted surface: Tech. rep.*, West Conshohocken, PA: ASTM International, <http://dx.doi.org/10.1520/G0173-03R20>.
- Berardi, U. (2015). The development of a monolithic aerogel glazed window for an energy retrofitting project. *Applied Energy*, 154, 603–615. <http://dx.doi.org/10.1016/j.apenergy.2015.05.059>.
- Bilardo, M., Fraisse, G., Pailha, M., & Fabrizio, E. (2019). Modelling and performance analysis of a new concept of integral collector storage (ICS) with phase change material. *Solar Energy*, 183, 425–440. <http://dx.doi.org/10.1016/j.solener.2019.03.032>.
- Borri, E., Zsebinszki, G., & Cabeza, L. (2021). Recent developments of thermal energy storage applications in the built environment: A bibliometric analysis and systematic review. *Applied Thermal Engineering*, 189, <http://dx.doi.org/10.1016/j.applthermaleng.2021.116666>.
- Bournas, I. (2020). Daylight compliance of residential spaces: Comparison of different performance criteria and association with room geometry and urban density. *Building and Environment*, 185, <http://dx.doi.org/10.1016/j.buildenv.2020.107276>.
- Cabeza, L., & Chàfer, M. (2020). Technological options and strategies towards zero energy buildings contributing to climate change mitigation: A systematic review. *Energy and Buildings*, 219, <http://dx.doi.org/10.1016/j.enbuild.2020.110009>.
- Cai, W., Yue, J., Dai, Q., Hao, L., Lin, Y., Shi, W., et al. (2018). The impact of room surface reflectance on corneal illuminance and rule-of-thumb equations for circadian lighting design. *Building and Environment*, 141, 288–297. <http://dx.doi.org/10.1016/j.buildenv.2018.05.056>.
- Capelletti, R. (2017). Luminescence. In *Reference module in materials science and materials engineering*. Elsevier, <http://dx.doi.org/10.1016/B978-0-12-803581-8.01247-9>.
- Chen, C., & Shi, J. (1998). Metal chelates as emitting materials for organic electroluminescence. *Coordination Chemistry Reviews*, 171, 161–174. [http://dx.doi.org/10.1016/S0010-8545\(98\)90027-3](http://dx.doi.org/10.1016/S0010-8545(98)90027-3).
- Cheung, P., & Jim, C. (2019). Effects of urban and landscape elements on air temperature in a high-density subtropical city. *Building and Environment*, 164, <http://dx.doi.org/10.1016/j.buildenv.2019.106362>.
- Chiatti, C., Fabiani, C., Cotana, F., & Pisello, A. L. (2021). Exploring the potential of photoluminescence for urban passive cooling and lighting applications: a new approach towards materials' optimization. *Energy*, 231, <http://dx.doi.org/10.1016/j.energy.2021.120815>.
- Chiatti, C., Fabiani, C., & Pisello, A. L. (2021). Long persistent luminescence: A road map toward promising future developments in energy and environmental science. *Annual Review of Materials Research*, 51(1), <http://dx.doi.org/10.1146/annurev-matsci-091520-011838>.
- DIAL GmbH, DIALux. URL <https://www.dialux.com/en-GB/dialux>.
- Dimoudi, A., Zoras, S., Kantioura, A., Stogiannou, X., Kosmopoulos, P., & Pallas, C. (2014). Use of cool materials and other bioclimatic interventions in outdoor places in order to mitigate the urban heat island in a medium size city in Greece. *Sustainable Cities and Society*, 13, 89–96. <http://dx.doi.org/10.1016/j.scs.2014.04.003>.
- EN12464-1:2011 (2011). *Light and lighting - Lighting of work places - Part 1: Indoor work places: Tech. rep.*, CEN (European Committee for Standardization).
- Fabiani, C., Chiatti, C., & Pisello, A. L. (2021). Development of photoluminescent composites for energy efficiency in smart outdoor lighting applications: An experimental and numerical investigation. *Renewable Energy*, 172, 1–15. <http://dx.doi.org/10.1016/j.renene.2021.02.071>.
- Fan, Z., Yang, Z., & Yang, L. (2020). Daylight performance assessment of atrium skylight with integrated semi-transparent photovoltaic for different climate zones in China. *Building and Environment*, Article 107299. <http://dx.doi.org/10.1016/j.buildenv.2020.107299>.
- Gao, T., Ihara, T., Grynning, S., Jelle, B., & Lien, A. (2016). Perspective of aerogel glazings in energy efficient buildings. *Building and Environment*, 95, 405–413. <http://dx.doi.org/10.1016/j.buildenv.2015.10.001>.
- Garnier, C., Muneer, T., & McCauley, L. (2015). Super insulated aerogel windows: Impact on daylighting and thermal performance. *Building and Environment*, 94(P1), 231–238. <http://dx.doi.org/10.1016/j.buildenv.2015.08.009>.
- Gilbert, H., Mandel, B., & Levinson, R. (2016). Keeping California cool: Recent cool community developments. *Energy and Buildings*, 114, 20–26. <http://dx.doi.org/10.1016/j.enbuild.2015.06.023>.
- Gilbert, H., Rosado, P., Ban-Weiss, G., Harvey, J., Li, H., Mandel, B., et al. (2017). Energy and environmental consequences of a cool pavement campaign. *Energy and Buildings*, 157, 53–77. <http://dx.doi.org/10.1016/j.enbuild.2017.03.051>.
- Giovannini, L., Goia, F., Lo Verso, V., & Serra, V. (2017). Phase change materials in glazing: Implications on light distribution and visual comfort. Preliminary results. *Energy Procedia*, 111, 357–366. <http://dx.doi.org/10.1016/j.egypro.2017.03.197>.
- Gong, X., Pan, Y., Xie, X., Tong, T., Chen, R., & Gao, D. (2018). Synthesis, characterization and electroluminescence of two highly-twisted non-doped blue light-emitting materials. *Optical Materials*, 78, 94–101. <http://dx.doi.org/10.1016/j.optmat.2018.02.012>.
- Gros, A., Bonzonnet, E., & Inard, C. (2014). Cool materials impact at district scale—Coupling building energy and microclimate models. *Sustainable Cities and Society*, 13, 254–266. <http://dx.doi.org/10.1016/j.scs.2014.02.002>.
- Havasi, V., Sipos, G., Konya, Z., & Kukovec, A. (2020). Luminescence and color properties of Ho³⁺ co-activated Sr₄Al₁₄O₂₅:Eu²⁺, Dy³⁺ phosphors. *Journal of Luminescence*, 220, <http://dx.doi.org/10.1016/j.jlumin.2019.116980>.
- He, B.-J., Wang, J., Liu, H., & Ulpiani, G. (2021). Localized synergies between heat waves and urban heat islands: Implications on human thermal comfort and urban heat management. *Environmental Research*, 193, <http://dx.doi.org/10.1016/j.envres.2020.110584>.
- Kahlke, T., & Umbers, K. (2016). Bioluminescence. *Current Biology : CB*, 26(8), R313–R314. <http://dx.doi.org/10.1016/j.cub.2016.01.007>.
- Kousis, I., Fabiani, C., Gobbi, L., & Pisello, A. (2020). Phosphorescent-based pavements for counteracting urban overheating – A proof of concept. *Solar Energy*, 202, 540–552. <http://dx.doi.org/10.1016/j.solener.2020.03.092>.
- Leloup, F., Leyre, S., Bauwens, E., Abebe, T., & Hanselaer, P. (2015). Design of an inexpensive integrating sphere student laboratory setup for the optical characterization of light sources. *European Journal of Physics*, 37(1), <http://dx.doi.org/10.1088/0143-0807/37/1/015302>.
- Levinson, R., Chen, S., Ferrari, C., Berdahl, P., & Slack, J. (2017). Methods and instrumentation to measure the effective solar reflectance of fluorescent cool surfaces. *Energy and Buildings*, 152, 752–765. <http://dx.doi.org/10.1016/j.enbuild.2016.11.007>.
- Mohajeri, N., Gudmundsson, A., Kunckler, T., Upadhyay, G., Assouline, D., Kämpf, J., et al. (2019). A solar-based sustainable urban design: The effects of city-scale street-canyon geometry on solar access in Geneva, Switzerland. *Applied Energy*, 240, 173–190. <http://dx.doi.org/10.1016/j.apenergy.2019.02.014>.
- Moline, M., Blackwell, S., Case, J., Haddock, S., Herren, C., Orrico, C., et al. (2009). Bioluminescence to reveal structure and interaction of coastal planktonic communities. *Deep-Sea Research Part II: Topical Studies in Oceanography*, 56(3–5), 232–245. <http://dx.doi.org/10.1016/j.dsr2.2008.08.002>.
- Ohno, Y. (1998). Detector-based luminous-flux calibration using the Absolute Integrating-Sphere Method. *Metrologia*, 35(4), 473–478. <http://dx.doi.org/10.1088/0026-1394/35/4/45>.
- Peeters, S., Smolders, K., & de Kort, Y. (2020). What you set is (not) what you get: How a light intervention in the field translates to personal light exposure. *Building and Environment*, 185, <http://dx.doi.org/10.1016/j.buildenv.2020.107288>.
- Pigliatulle, I., Chàfer, M., Pisello, A., Pérez, G., & Cabeza, L. (2020). Inter-building assessment of urban heat island mitigation strategies: Field tests and numerical modelling in a simplified-geometry experimental set-up. *Renewable Energy*, 147, 1663–1675. <http://dx.doi.org/10.1016/j.renene.2019.09.082>.
- Qi, J., He, B., Wang, M., Zhu, J., & Fu, W. (2019). Do grey infrastructures always elevate urban temperature? No, utilizing grey infrastructures to mitigate urban heat island effects. *Sustainable Cities and Society*, 46, Article 101392. <http://dx.doi.org/10.1016/j.scs.2018.12.020>.
- Resch, E., Andresen, I., Cherubini, F., & Brattebø, H. (2021). Estimating dynamic climate change effects of material use in buildings—Timing, uncertainty, and emission sources. *Building and Environment*, 187, <http://dx.doi.org/10.1016/j.buildenv.2020.107399>.
- Rosso, F., Fabiani, C., Chiatti, C., & Pisello, A. (2019). Cool, photoluminescent paints towards energy consumption reductions in the built environment. *Journal of Physics: Conference Series*, 1343(1), <http://dx.doi.org/10.1088/1742-6596/1343/1/012198>.
- Rosso, F., & Pisello, A. (2018). Outdoor living: the impact of urban materials and morphology on pedestrians thermal and visual comfort— a state of the art review and discussion. In *42nd IAHS 2018 World Congr. Hous.*
- Rosso, F., Pisello, A., Cotana, F., & Ferrero, M. (2017). Cool, translucent natural envelope: Thermal-optics characteristics experimental assessment and thermal-energy and day lighting analysis. *Energy Procedia*, 111, 578–587. <http://dx.doi.org/10.1016/j.egypro.2017.03.220>.
- Santamouris, M., & Yun, G. (2020). Recent development and research priorities on cool and super cool materials to mitigate urban heat island. *Renewable Energy*, 161, 792–807. <http://dx.doi.org/10.1016/j.renene.2020.07.109>.
- Singh, V., Hakeem, D., & Lakshminarayana, G. (2020). An insight into the luminescence properties of Ce³⁺ in garnet structured CaY₂Al₄SiO₁₂:Ce³⁺ phosphors. *Optik*, 206, <http://dx.doi.org/10.1016/j.ijleo.2019.163833>.
- Smith, T., & Guild, J. (1931). The C.I.E. colorimetric standards and their use. *Transactions of the Optical Society*, 33(3), 73–134. <http://dx.doi.org/10.1088/1475-4878/33/3/301>.
- Tan, X., Sun, X., Huang, C., Yuan, Y., & Hou, D. (2021). Comparison of cooling effect between green space and water body. *Sustainable Cities and Society*, 67, Article 102711. <http://dx.doi.org/10.1016/j.scs.2021.102711>.
- Tepanosyan, G., Muradyan, V., Hovsepian, A., Pinigin, G., Medvedev, A., & Asmaryan, S. (2021). Studying spatial-temporal changes and relationship of land cover and surface Urban Heat Island derived through remote sensing in Yerevan, Armenia. *Building and Environment*, 187, <http://dx.doi.org/10.1016/j.buildenv.2020.107390>.

- Ulpiani, G. (2021). On the linkage between urban heat island and urban pollution island: Three-decade literature review towards a conceptual framework. *Science of the Total Environment*, 751, <http://dx.doi.org/10.1016/j.scitotenv.2020.141727>.
- Xu, X., & Asawa, T. (2020). Systematic numerical study on the effect of thermal properties of building surface on its temperature and sensible heat flux. *Building and Environment*, 168, <http://dx.doi.org/10.1016/j.buildenv.2019.106485>.
- Yousif, A., Abas, B., Shivaramu, N., & Swart, H. (2020). Structural and luminescence properties of Y₂O₃:Eu³⁺ red phosphor by incorporation of Ga³⁺ and Bi³⁺ ions. *Materials Research Bulletin*, 124, <http://dx.doi.org/10.1016/j.materresbull.2019.110752>.
- Zhao, T., & Fong, K. (2017). Characterization of different heat mitigation strategies in landscape to fight against heat island and improve thermal comfort in hot-humid climate (Part II): Evaluation and characterization. *Sustainable Cities and Society*, 35, 841–850. <http://dx.doi.org/10.1016/j.scs.2017.05.006>.